
# "Theory and numerical analysis of the Mathieu functions"

by

Dr. Julio César Gutiérrez Vega
Photonics and Mathematical Optics Group

http://homepages.mty.itesm.mx/jgutierr/
e-mail: juliocesar@itesm.mx

Monterrey, NL, México
March, 2003

# Contents

# List of Figures

# Chapter 1

# Introduction

## 1.1 Elliptical-cylindrical coordinate system

In this section we introduce the elliptic coordinates. As we will see, this coordinate system is closely related to circular-cylinder system, and in some circumstances the latter could be considered as a special case of the former as we will see later.

Let us consider an ellipse in the plane $(x, y)$ whose equation reads $(x/a)^2 + (y/b)^2 = 1$, where $a > b$. The semi-focal distance $f$ is given by $f^2 = a^2 - b^2$, and the eccentricity $e$ reads as $e = f/a$, $e \in [0, 1]$. The ellipse is defined by any pair of parameters selected from $\{a, b, f, e\}$.

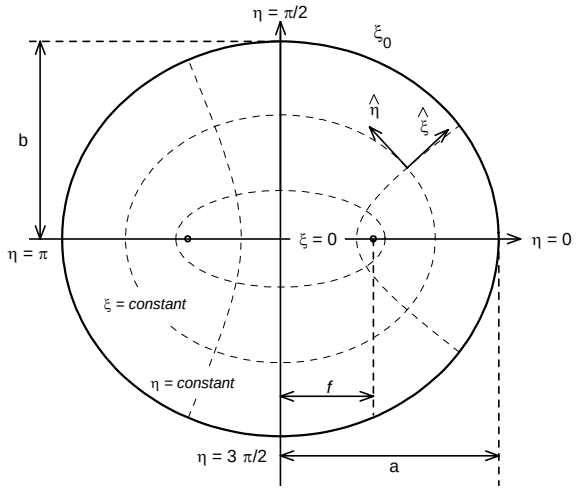


Figure 1-1: Elliptical-cylinder coordinate system.

The elliptic coordinates $(\xi, \eta, z)$ are defined according to the transformation $(x + iy) = f \cosh(\xi + i\eta)$. Now,

by equating the real and the imaginary parts of each side we obtain

$$x = f\cosh\xi\cos\eta; \qquad y = f\sinh\xi\sin\eta; \qquad z = z, \tag{1.1}$$

where $\xi$ works as a radial coordinate and takes the values $\xi \in [0,\infty)$, the coordinate $\eta$ is an angular coordinate taking the range $\eta \in [0, 2\pi)$, and $z \in (-\infty, \infty)$. The surface $\xi = \xi_0$ reduces to the elliptic cylinder

$$\left[\frac{x}{f\cosh\xi_0}\right]^2 + \left[\frac{y}{f\sinh\xi_0}\right]^2 = \cos^2\eta + \sin^2\eta = 1, \tag{1.2}$$

with semi-major axis $a = f\cosh\xi_0$, and semi-minor axis $b = f\sinh\xi_0$, see Fig. 1-1. The surface $\eta = \eta_0$ reduces to the hyperbolic cylinder

$$\left[\frac{x}{f\cos\eta_0}\right]^2 - \left[\frac{y}{f\sin\eta_0}\right]^2 = \cosh^2\xi - \sinh^2\xi = 1. \tag{1.3}$$

which crosses the $x$-axis at $\pm f\cos\eta_0$ and has asymptotes $y = \pm(\tan\eta_0)\,x$.

The two families of conics are confocal, intersect orthogonally, and each intersection $(\xi,\eta)$ corresponds to a point in the plane $(x,y)$ defined by Eqs. (1.1). Observe in Fig. 1-1 that for $\eta = 0$ the hyperbola degenerates to the line segment $y = 0$, $x \geq f$. For $\eta = \pi$ the hyperbola degenerates to the line segment $y = 0$, $x \leq -f$. For $\eta = \pi/2$ the hyperbola becomes the positive $y$-axis, whereas $\eta = 3\pi/2$ becomes the negative $y$-axis

In Fig. 1-1 we appreciate that confocal ellipses collapse to a segment of straight line joining the two foci when $\xi = 0$. The focal points $(x,y) = (\pm f, 0)$ are located in the elliptic plane on $(\xi,\eta) = (0,0)$ and $(0,\pi)$. Finally the origin of the coordinate system can be specified with $(\xi,\eta) = (0,\pi/2)$ or $(0, 3\pi/2)$.

The transition to the circular case occurs in the limit when $f$ tends to zero and $\xi$ tends to infinite. The distance $\rho$ of any point $(\xi,\eta)$ in the plane $(x,y)$ to the origin is found combining Eqs.(1.1), $\rho^2 = x^2 + y^2 = f^2\cosh^2\xi\cos^2\eta + f^2\sinh^2\xi\sin^2\eta$. When $\xi$ increases then $\sinh\xi \to \cosh\xi$, so we can factorize $\cosh\xi$ to obtain the radius

$$\rho|_{\xi\ \text{large}} \sim f\cosh\xi \sim \frac{f\exp\xi}{2}.$$

This expression is important to observe that the confocal ellipses sketched in Fig. 1-1 tend to circles when $\xi$ is large. In the same fashion the azimuthal angle $\varphi$ of any point $(\xi,\eta)$ with respect to the $x$-axis reads as

$$\varphi = \arctan\left(\frac{y}{x}\right) = \arctan\left(\frac{f\sinh\xi\sin\eta}{f\cosh\xi\cos\eta}\right),$$

which reduces to $\varphi \sim \eta$ for large $\xi$. Now it is evident that the variable $\eta$ plays a role identical to an azimuthal angle, and $f\exp(\xi)/2$ is similar to a radial variable.

The description of the elliptic coordinate system is not complete without introducing the corresponding scale factors.

$$h \equiv h_\xi = h_\eta = f\sqrt{\cosh^2\xi - \cos^2\eta} = f\sqrt{\frac{1}{2}(\cosh 2\xi - \cos 2\eta)}; \qquad h_z = 1. \tag{1.4}$$

We will use the scale factors in the next sections to find the nabla and Laplacian operators in elliptic coordinates.

## 1.2 Wave and Helmholtz equations in elliptic coordinates

With the elliptic coordinates introduced in last section we express the three-dimensional wave equation in elliptic coordinates and apply the method of SoV to separate it into four ordinary differential equations. We start our analysis from the scalar wave equation

$$\left[\nabla^2 - \frac{1}{v^2}\frac{\partial^2}{\partial t^2}\right] U\left(\mathbf{r}\,,t\right) = 0, \tag{1.5}$$

where $v$ is a constant with units of velocity $[m/s]$ and which takes different expressions depending on the phenomenon to be described (*e.g.* $v^{-2} = \mu\epsilon$ for electromagnetic fields). By assuming a solution of the form $U\left(\mathbf{r}\,,t\right) = U\left(\mathbf{r}\right)T\left(t\right)$ and replacing it into Eq. (1.5) we obtain

$$\left[\frac{d^2}{dt^2} + k^2v^2\right] T\left(t\right) = 0, \tag{1.6}$$

$$\left[\nabla^2 + k^2\right] U\left(\mathbf{r}\right) = 0, \tag{1.7}$$

where $-k^2$ is the constant of separation. Eq. (1.6) is the *Harmonic equation* whose solutions are $T\left(t\right) = \exp\left(\pm i\omega t\right)$, where $\omega = kv$. Eq. (1.7) is in fact the 3-D Helmholtz equation. In general, for cylindrical systems the Laplacian operator takes the form $\nabla^2 = \nabla_t^2 + \partial^2/\partial z^2$, then assuming a spatial solution $U\left(\mathbf{r}\right) = U_t\left(\mathbf{r}_t\right)Z\left(z\right)$ we separate Eq. (1.7) into

$$\left[\frac{d^2}{dz^2} + k_z^2\right] Z\left(z\right) = 0, \tag{1.8}$$

$$\left[\nabla_t^2 + k_t^2\right] U_t\left(\mathbf{r}_t\right) = 0, \tag{1.9}$$

where $k_z^2$ is the constant of separation and $k_t^2 = k^2 - k_z^2$. Eq. (1.8) is again the Harmonic equation whose solutions are $Z\left(z\right) = \exp\left(\pm ik_z z\right)$. Finally we recognize that Eq. (1.9) is the two-dimensional Helmholtz equation. By replacing the scale factors in elliptic coordinates Eq. (1.4) into the transverse Laplacian $\nabla_t^2 = \left(1/h_\xi^2\right)\partial^2/\partial\xi^2 + \left(1/h_\eta^2\right)\partial^2/\partial\eta^2$ and taking $\mathbf{r}_t = (\xi,\eta)$ we obtain the 2-D Helmholtz equation in elliptic coordinates

$$\left[\frac{\partial^2}{\partial\xi^2} + \frac{\partial^2}{\partial\eta^2} + \frac{f^2k_t^2}{2}\left(\cosh 2\xi - \cos 2\eta\right)\right] U_t\left(\xi,\eta\right) = 0. \tag{1.10}$$

Applying again the technique of SoV we assume a solution of the form $U_t\left(\xi,\eta\right) = R(\xi)\Theta(\eta)$. Substitution of

$U_t$ into Eq. (1.10) yields

$$\left[\frac{d^2}{d\xi^2} - (a - 2q\cosh 2\xi)\right] R(\xi) = 0, \tag{1.11}$$

$$\left[\frac{d^2}{d\eta^2} + (a - 2q\cos 2\eta)\right] \Theta(\eta) = 0, \tag{1.12}$$

where $a$ is the constant of separation, and $q$ is a dimensionless parameter related to the transverse propagation constant $k_t$ by

$$q \equiv \frac{f^2}{4} k_t^2. \tag{1.13}$$

Equations (1.11) and (1.12) are known in Physics and Engineering as the *Radial Mathieu Equation* (RME), and the *Angular Mathieu Equation* (AME) respectively. Their solutions are the *Radial Mathieu Functions* (RMFs) and the *Angular Mathieu Functions* (AMFs).

It is important to mention that in the Mathematics jargon Eqs. (1.11) and (1.12) are often referred to as *Modified* and *Ordinary Mathieu Equations*. Throughout this thesis we will use the Radial and Angular terminology by virtue of its physical meaning in relation with wave propagation.

The principal properties of the Mathieu functions will be described in detail in the next Chapter. To finish this section we recollect all partial solutions to write the general solution of the scalar wave equation in elliptic coordinates as

$$U(\mathbf{r}, t) = R(\xi)\Theta(\eta) \exp(\pm i k_z z \pm i\omega t).$$

This solution represents a transverse field distribution $R(\xi)\Theta(\eta)$ propagating in $z$ direction with a phase velocity $v_p = \omega/k_z$.

# Chapter 2

# Theory of the elliptic-cylinder functions

The elliptical-cylinder Mathieu functions were introduced by Emile Mathieu in 1868, as the result of investigating the vibrating modes in an elliptic membrane [36, 54]. Despite a considerable amount of analytical knowledge of Mathieu functions, there are few textbooks which include a treatment about its theory [1, 33, 27, 53, 56, 57, 69, 75], and practically there is none which discusses details regarding to its programming. This lack of literature is perhaps because at least five different nomenclatures are actually in use [1], due to the limited number of applications [62], and by virtue of the mathematical difficulties to compute the Mathieu functions.

This chapter is intended to review the theory of the Angular and Radial Mathieu functions of integral order. We strongly emphasize the aspects concerning the calculation of the characteristic numbers and the coefficients of the series, because their high accuracy is the key to get a successful evaluation of the Mathieu functions. For the sake of brevity, several procedures and important identities are given in Appendix A. We omit the topics relative to integral equations, so we refer the interested reader to specialized references [1, 33, 53, 56, 57, 69, 75]. The numerical analysis and typical plots of the Mathieu functions are reserved for Chapter 3.

## 2.1 Mathieu differential equations

The canonical form of the Angular (*i.e.* Ordinary) and the Radial (*i.e.* Modified) Mathieu equations read

$$\left[\frac{d}{d\eta^2} + (a - 2q\cos 2\eta)\right]\Theta(\eta) = 0, \tag{2.1}$$

$$\left[\frac{d}{d\xi^2} - (a - 2q\cosh 2\xi)\right]R(\xi) = 0, \tag{2.2}$$

where $a$ is a separation constant, and $q$ is related to the transverse spatial frequency $k_t$ by Eq. (1.13). For the moment, the constants $a$ and $q$ will be limited to real numbers, but $\eta$ and $\xi$ are unrestricted. It is a fortunate circumstance that Eq. (2.1) transforms into Eq. (2.2), and vice versa, if $\eta$ is replaced by $\pm i\xi$. The solutions of Eq. (2.1) are the Angular Mathieu Functions (AMFs), whereas the solutions of Eq. (2.2) are the Radial Mathieu

Functions (RMFs).

The canonical form Eq. (2.1) was introduced first by Ince [43], however there is not a generally accepted form. For example Whittaker [75] put $q = -8q$, and Stratton [69] and Morse [57] have $a = b - c^2/2$, $q = c^2/4$. Some authors that used the form of Eq. (2.1) were Refs. [1, 27, 33, 56].

The two most common notational conventions for Mathieu functions are those of Whittaker-McLachlan [56] and Stratton-Morse [57, 69]. The nomenclature of McLachlan had its origins in the notation used by the first researchers of the Mathieu functions and it is, in certain way, arbitrary. This arbitrariness in the notation, united to the existence of different nomenclatures and normalizations, often leads to have a confused panorama of the theory of Mathieu functions. Despite this fact, the McLachlan's terminology is the most employed notation in scientific literature.

On the other side, the Stratton nomenclature was created thinking in the connection of each Mathieu function with its corresponding Bessel analogy. From this point of view, the notation of Stratton is advantageous, since it facilitates the visualization and classification of the Mathieu functions.

The crux of the divergence of opinion between the McLachlan and Stratton notations, is that they have associated different normalization schemes. Whereas McLachlan scales its Angular functions such that the normalization factor is always $\sqrt{\pi}$, Stratton normalizes in such a way that the even Angular functions and the derivative of the odd Angular functions have unit value at $\eta = 0$. Our own experience is that Stratton's scheme can produce, in some circumstances, very large values for the Angular functions, whereas McLachlan's scheme usually keeps the functions inside the range $[-1, 1]$.

In applications, the particular normalization adopted is of little importance, except possibly for obtaining quantitative relations between solutions of various types. It is worth noting, however, that normalizations differ only by a proportionally factor, thus conversion from one scheme to another is rather easy.

Throughout this thesis, we adopt the nomenclature introduced by Stratton because it is more intuitive and elegant, but we preserve the normalization used by McLachlan, since it is more practical for numerical purposes and applications. A useful table of comparative notations is provided by Abramowitz [1, Chap. 20].

## 2.2 Solution of the Angular Mathieu equation

In this section we study the procedure to solve the AME Eq. (2.1). Physical considerations are usually such that AME Eq. (2.1) has periodic solutions with period $\pi$ or $2\pi$. The values of $a$ which satisfy this condition are known as *characteristic values* (eigenvalues), and they generate an infinite set of real values which have the property $a_0 < a_1 < a_2 < \cdots$. When the solutions $\Theta(\eta)$ are even with respect to $\eta = 0$, the characteristic values are denoted as $a_m(q) : m \in \{0, 1, 2, \cdots\}$, whereas for odd solutions they are represented as $b_m(q) : m \in \{1, 2, 3, \cdots\}$.

The characteristic values play an important role since they define the stability of the solutions. A solution is defined to be stable if it tends to zero or remains bounded as $\eta \to \infty$. A solution is defined to be unstable if it tends to $\pm\infty$ as $\eta \to \infty$. A solution with period $\pi$ or $2\pi$ is said to be neutral, but may be regarded as a special

case of a stable solution. In particular for Mathieu functions, when the eigenvalues $a$ belong to a discrete set, we say that the solutions are of *integral order*, otherwise they are of *fractional order*. The functions of integral order are always stable, but those of fractional order can be stable or unstable.

Since AME Eq. (2.1) is a second-order differential equation, there are two families of independent solutions, see Fig. 2-1. The functions *ce* and *se* corresponds to the first kind solutions and they are periodic. The notation *ce* and *se* comes from *cosine-elliptic* and *sine-elliptic,* and it was first suggested by Whittaker and Watson [75]. Nowadays it is a widely accepted notation for the Angular Mathieu functions.

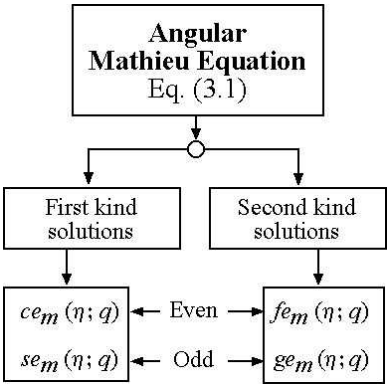


Figure 2-1: Classification of the Angular Mathieu functions.

On the other side, the functions $fe$ and $ge$ are the solutions of the second kind and they are non periodic. The *'f'* and the *'g'* occurring in $fe$ and $ge$ were arbitrarily defined by Ince [43]. Not being periodic, they will rarely be of importance in applications, therefore, in this work we will restrict ourselves to solve the first kind solutions.

As we mentioned above, the constant $a$ in Eq. (2.1) is not given *a priori,* and we have to consider how it is to be determined. In most of the physical problems, Eq. (2.1) describes the *angular* dependence of a physical quantity (*e.g.* electric or magnetic field), and therefore, its solutions must be periodic with period $2\pi$. These periodic solutions can be expressed by using the Fourier series, and they fall into four classes, according to their symmetry or antisymmetry, about $\eta = 0$ and $\eta = \pi/2$.

$$\text{Class I} \quad : \qquad ce_{2n}(\eta;q) = \sum_{j=0}^{\infty} A_{2j}(q)\cos 2j\eta, \qquad :(a_{2n}) \tag{2.3}$$

$$\text{Class II} \quad : \qquad ce_{2n+1}(\eta;q) = \sum_{j=0}^{\infty} A_{2j+1}(q)\cos(2j+1)\eta, \qquad :(a_{2n+1}) \tag{2.4}$$

$$\text{Class III} \quad : \qquad se_{2n+2}(\eta;q) = \sum_{j=0}^{\infty} B_{2j+2}(q)\sin(2j+2)\eta, \qquad :(b_{2n+2}) \tag{2.5}$$

$$\text{Class IV} \quad : \qquad se_{2n+1}(\eta;q) = \sum_{j=0}^{\infty} B_{2j+1}(q)\sin(2j+1)\eta, \qquad :(b_{2n+1}) \tag{2.6}$$

where $n \in \{0, 1, 2, \cdots\}$, and the symbols in the right column denote the corresponding characteristic values. The

coefficients $A$ and $B$ depends on the parameter $q$, and we will study the procedure to find them in the next subsections.

### 2.2.1 Recurrence relations for the coefficients

If we substitute Eqs. (2.3)-(2.6) in (2.1) we obtain the following recurrence relations for the Fourier coefficients for a given characteristic value $a_m$ or $b_m$. For simplicity the detailed procedure is shown in Appendix A.

Class I: $ce_{2n}$, $(a = a_{2n})$

$$aA_0 - qA_2 = 0, \tag{2.7a}$$

$$(a-4)A_2 - q(2A_0 + A_4) = 0, \tag{2.7b}$$

$$\left[a-(2j)^2\right]A_{2j} - q(A_{2j-2} + A_{2j+2}) = 0, \qquad j \in \{2,3,\cdots\} \tag{2.7c}$$

Class II: $ce_{2n+1}$, $(a = a_{2n+1})$

$$(a-1)A_1 - q(A_1 + A_3) = 0, \tag{2.8a}$$

$$\left[a-(2j+1)^2\right]A_{2j+1} - q(A_{2j-1} + A_{2j+3}) = 0, \qquad j \in \{1,2,\cdots\} \tag{2.8b}$$

Class III: $se_{2n+2}$, $(b = b_{2n+2})$

$$(b-4)B_2 - qB_4 = 0, \tag{2.9a}$$

$$\left[b-(2j)^2\right]B_{2j} - q(B_{2j-2} + B_{2j+2}) = 0, \qquad j \in \{2,3,\cdots\} \tag{2.9b}$$

Class IV: $se_{2n+1}$, $(b = b_{2n+1})$

$$(b-1)B_1 - q(B_3 - B_1) = 0, \tag{2.10a}$$

$$\left[b-(2j+1)^2\right]B_{2j+1} - q(B_{2j-1} + B_{2j+3}) = 0, \qquad j \in \{1,2,\cdots\} \tag{2.10b}$$

The recurrence relations Eqs. (2.7)-(2.10) are linear difference equations, and their convergence is important for numerical purposes, since it determines the precision of the Fourier coefficients. Let us analyze the characteristics of the recurrence relations. By substituting the definitions

$$G_{2j} \equiv \frac{A_{2j}}{A_{2j-2}}, \qquad V_j \equiv \frac{a-j^2}{q}$$

into Eq. (2.7c), we obtain

$$G_{2j+2} + \frac{1}{G_{2j}} = \frac{a-(2j)^2}{q} = V_{2j} \tag{2.11}$$

where we can conclude that

1) $G_{2j+2} + 1/G_{2j} \to -\infty$ monotonically, since $V_{2j} \to -\infty$ as $j \to \infty$.

2) In order that $G_{2j+2} + 1/G_{2j} \to -\infty$, then it must be satisfied $G_{2j} \to 0^-$ or $G_{2j} \to -\infty$.

3) $G_{2j}$ cannot tend to $-\infty$, because then $|A_{2j}| > |A_{2j-2}|$, and the solution is unstable. Therefore $G_{2j} \to 0^-$, which assures that $A_{2j} \to 0$ as $j \to \infty$.

4) Since $G_{2j}$ must be negative, then $A_{2j}$ and $A_{2j-2}$ have opposite signs each other. Consequently the magnitude of the coefficients decreases, and their signs alternate as $j$ increases.

Eq. (2.11) can be rewritten as

$$\left[a-(2j)^2\right] - q\left(\frac{1+G_{2j+2}G_{2j}}{G_{2j}}\right) = 0.$$

Since $G_{2j} \to 0$ as $j$ increases, when $j$ is large enough we can assume $G_{2j+2}G_{2j} \ll 1$, and $a \ll (2j)^2$, then

$$|G_{2j}| \equiv \left|\frac{A_{2j}}{A_{2j-2}}\right| \sim \frac{q}{(2j)^2} \to 0, \qquad \text{as } j \to +\infty,$$

where we can shift the index to obtain the relation

$$\left|\frac{A_{2j+2}}{A_{2j}}\right| \sim \frac{q}{(2j+2)^2} \to 0, \qquad \text{as } j \to +\infty, \tag{2.12}$$

which will be very useful in the next chapter to estimate the upper value of $j$ in order to truncate the series for a given accuracy.

### 2.2.2 Characteristic values $a_m$ and $b_m$

In order to solve the recurrence relations (7-10), we need first to find the characteristic values $a_m$ and $b_m$. We start from Eq. (2.11), by solving $G_{2j}$ we get

$$G_{2j} = \frac{1}{V_{2j} - G_{2j+2}},$$

applying again the above relation to $G_{2j+2}$ we obtain

$$G_{2j} = \frac{1}{V_{2j} - \frac{1}{V_{2j+2} - G_{2j+4}}}, \qquad j \in \{2, 3, \cdots\}$$

and so forth we construct the continued fraction

$$G_4 = \frac{1}{V_4 -}\frac{1}{V_6 -}\frac{1}{V_8 -}\frac{1}{V_{10} - \cdots}, \tag{2.13}$$

where we have used the notation [58]

$$\frac{1}{g_1 -}\frac{1}{g_2 -}\frac{1}{g_3 - \cdots} = \frac{1}{g_1 - \frac{1}{g_2 - \frac{1}{g_3 - \cdots}}}.$$

On the other hand, Eqs. (2.7a) and (2.7b) can be rewritten as

$$G_2 = V_0, \quad \text{and} \quad G_4 = V_2 - \frac{2}{G_2}, \tag{2.14}$$

respectively. By equating Eqs. (2.13) and (2.14)

$$G_4 = V_2 - \frac{2}{G_2} = V_2 - \frac{2}{V_0} = \frac{1}{V_4 -}\frac{1}{V_6 -}\frac{1}{V_8 -}\frac{1}{V_{10} - ....},$$

we finally can write

$$\text{Class I} \qquad V_0 = \frac{2}{V_{2-}}\frac{1}{V_{4-}}\frac{1}{V_{6-}}..., \qquad (\text{Roots} = \alpha_{2n}) \tag{2.15}$$

The preceding continued fraction is an equation for $a$. Its roots are in fact the characteristic values $a_{2n}$ of the functions $ce_{2n}$. In the same manner the continued fractions for the remaining recurrence relations can be obtained.

$$\text{Class II} \qquad V_1 - 1 = \frac{1}{V_{3-}}\frac{1}{V_{5-}}\frac{1}{V_{7-}}..., \qquad (\text{Roots} = \alpha_{2n+1}) \tag{2.16}$$

$$\text{Class III} \qquad V_2 = \frac{1}{V_{4-}}\frac{1}{V_{6-}}\frac{1}{V_{8-}}..., \qquad (\text{Roots} = b_{2n+2}) \tag{2.17}$$

$$\text{Class IV} \qquad V_1 + 1 = \frac{1}{V_{3-}}\frac{1}{V_{5-}}\frac{1}{V_{7-}}..., \qquad (\text{Roots} = b_{2n+1}) \tag{2.18}$$

The characteristic values may be calculated by solving the eigenvalues of a tridiagonal infinite matrix as well. The procedure to obtain this matrix starting from the recurrence relations Eqs. (7-10) is given in Appendix A. Once the characteristic values have been determined by solving Eqs. (2.15)-(2.18), the recurrence relations (2.7)-(2.10) should be applied to calculate the Fourier coefficients. Once the coefficients has been computed, the Mathieu functions are obtained by using the series (2.3)-(2.6).

### 2.2.3 Characteristic curves $a(q)$ and $b(q)$

As we mentioned previously, for a given value of $q$ there exists a set of characteristic values $a \in \{a_m, b_m\}$, which can be determined by the procedure described in the previous section. This fact allows us to construct plots for the characteristic values as a function of $q$. The characteristic curves $a_m(q)$ and $b(q)$ in the $(a, q)$-plane are shown

in Fig. 2-2. Some interesting conclusions are obtained by observing these curves.

- When $q > 0$ and large enough, the curves $a_m$ and $b_{m+1}$ approach and are mutually asymptotic.
- When $q < 0$ and large enough, then $a_{2n} \sim a_{2n+1}$ and $b_{2n+1} \sim b_{2n+2}$.
- When $q = 0$, then $a_m = b_m = m^2$, and we recover the degenerate circular case.
- The curves $a_{2n+1}(q)$ and $b_{2n+1}(q)$ are mutually symmetrical, *e.g.* $a_3$ and $b_3$.
- The curves $a_{2n}(q)$ and $b_{2n+2}(q)$ are symmetrical with respect to axis $q = 0$.
- Excepting the curve $a_0$, which is tangential to the $q$-axis at origin, all curves intersect this axis twice, one value of $q$ being positive and the other negative. For the functions of even order $ce_{2n}$ and $se_{2n+2}$, the zeros are equal, but opposite. The zeros of $ce_{2n+1}$ are equal but opposite to those of $se_{2n+1}$.
- Because the Mathieu equation has only one solution of type $ce_m$ or $se_{m+1}$ ($q \neq 0$), two characteristic curves cannot intersect.
- For a given $q > 0$, the characteristic values are ordered as $\{a_{2n}, b_{2n+1}, a_{2n+1}, b_{2n+2}\}$.
- For a given $q < 0$, the characteristic values are ordered as $\{a_{2n}, a_{2n+1}, b_{2n+1}, b_{2n+2}\}$

The $(a, q)$-plane is important because it defines the stability zones of the Mathieu functions. Let us assume that $a$ in Eq. (2.1) can take any arbitrary value. If $a$ lies in a white zone, then the solutions are stable, otherwise they are unstable.

### 2.2.4 Orthogonality and normalization

As a consequence of the orthogonality property of the sine and cosine series [42], the functions $ce_m$ and $se_{m+1}$ are also orthogonal functions. According to the McLachlan normalization the Angular Mathieu function satisfies the next relations.

$$\int_0^{2\pi} ce_m(\eta; q) ce_p(\eta; q) d\eta = \int_0^{2\pi} se_m(\eta; q) se_p(\eta; q) d\eta = \begin{cases} \pi, & \text{if } m = p \\ 0, & \text{if } m \neq p \end{cases} \tag{2.19}$$

After substitution of Eqs. (2.3)-(2.6) in (2.19) we can obtain the following normalization relations for the Fourier coefficients of $ce_{2n}$, $ce_{2n+1}$, $se_{2n+2}$, and $se_{2n+1}$ respectively

$$2A_0^2 + \sum_{j=1}^{\infty} (A_{2j})^2 = \sum_{j=0}^{\infty} (A_{2j+1})^2 = \sum_{j=0}^{\infty} (B_{2j+2})^2 = \sum_{j=0}^{\infty} (B_{2j+1})^2 = 1. \tag{2.20}$$

Eq. (2.20) assures that all coefficients are bounded such that $|A_j| \leq 1$ and $|B_j| \leq 1$.

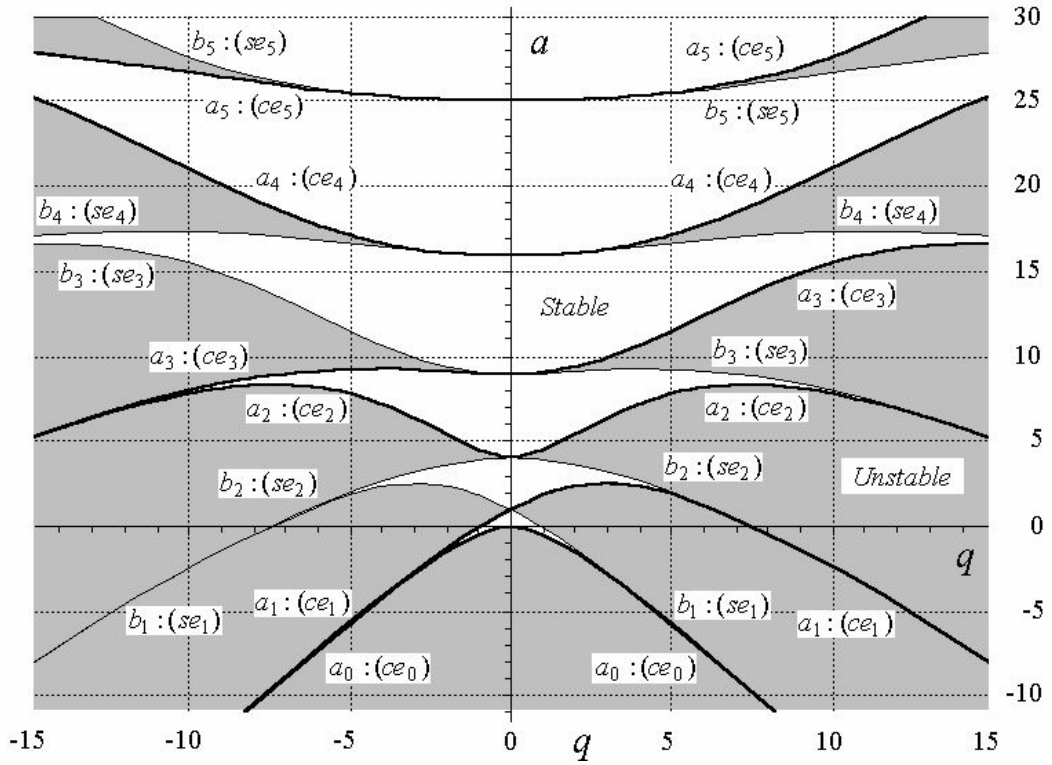


Figure 2-2: $(a, q)$ plane for Mathieu functions. The characteristic curves $a_0$, $b_1$, $a_1$, $b_2$, ... divide the plane into regions of stability and instability. The even-order curves are symmetrical, but the odd curves are asymmetrical about the $a$-axis. The chart was plotted by using the algorithms described in Chapter 4.

### 2.2.5 Asymptotic behavior of Angular solutions when $q \to 0$

When $q = 0$ the AME Eq. (2.1) becomes $\Theta'' + a\Theta = 0$, whose well-known solution is $\Theta(\eta) = A\cos\sqrt{a}\eta + B\sin\sqrt{a}\eta$, where $a > 0$, and $A$ and $B$ are arbitrary constants. In order to have $2\pi$-periodic solutions, $m = \sqrt{a} = 0, 1, 2, 3, \cdots$ must be satisfied. Thus the characteristic values when $q = 0$, read as $a_m \in \{0, 1, 4, 9, \cdots\}$. This result can be appreciated in $(a, q)$-plane, where we can see that $a_m = b_m$ for this special case as well.

As $q \to 0$, it is reasonable that Fourier series Eqs. (2.3)-(2.6) tend to $\cos m\eta$ or $\sin m\eta$. In order to ensure that this happens, all coefficients $A_j$ or $B_j$ must tend to zero, except $A_m$ or $B_m$ which must tend to unity. This result can be deduced from the recurrence relations. In fact in the limit when $q = 0$, Eqs. (7-8) simplify to

$$\left(a - j^2\right) A_j = 0, \qquad j \in \{0, 1, 2, \cdots\}$$

but $a = m^2$, thus $\left(a - j^2\right)$ vanish when $j = m$. This fact forces all coefficients $A_j \neq A_m$ to vanish. The only coefficient that can be different from zero is in fact $A_m$. To satisfy the normalization stated in Eq. (2.20) we should set $A_m = 1$.

### 2.2.6 Angular solutions with $q < 0$

If the sign of $q$ is changed, the ordinary solutions can be found by taking advantage of the properties of symmetry, namely

$$\begin{aligned}
ce_{2n}(\eta;-q) &= (-1)^n ce_{2n}(\pi/2-\eta;q), & fe_{2n}(\eta;-q) &= (-1)^{n+1} fe_{2n}(\pi/2-\eta;q),\\
ce_{2n+1}(\eta;-q) &= (-1)^n se_{2n+1}(\pi/2-\eta;q), & fe_{2n+1}(\eta;-q) &= (-1)^n ge_{2n+1}(\pi/2-\eta;q),\\
se_{2n+2}(\eta;-q) &= (-1)^n se_{2n+2}(\pi/2-\eta;q), & ge_{2n+2}(\eta;-q) &= (-1)^n ge_{2n+2}(\pi/2-\eta;q),\\
se_{2n+1}(\eta;-q) &= (-1)^n ce_{2n+1}(\pi/2-\eta;q), & ge_{2n+1}(\eta;-q) &= (-1)^n fe_{2n+1}(\pi/2-\eta;q),
\end{aligned} \tag{2.21}$$

## 2.3 Solution of the Radial Mathieu equation

The Radial Mathieu equation Eq. (2.2) plays in elliptic coordinates a similar role as the Bessel equation in circular coordinates. In this sense, for each Bessel function [$J$, $N$, $I$, and $K$] there exists a Radial Mathieu function, however the presence of even and odd versions in the elliptic case leads to eight RMFs. This abundance of elliptic solutions has provoked embroiled notations in literature which often complicates the recognition of the RMFs and their relations. In order to provide an overview of the whole family of Radial Mathieu functions and relate each one with its corresponding Bessel analogy, in Fig. 2-3 we show a graphical classification of the RMFs. As we explained earlier, the notation of Stratton is adopted.

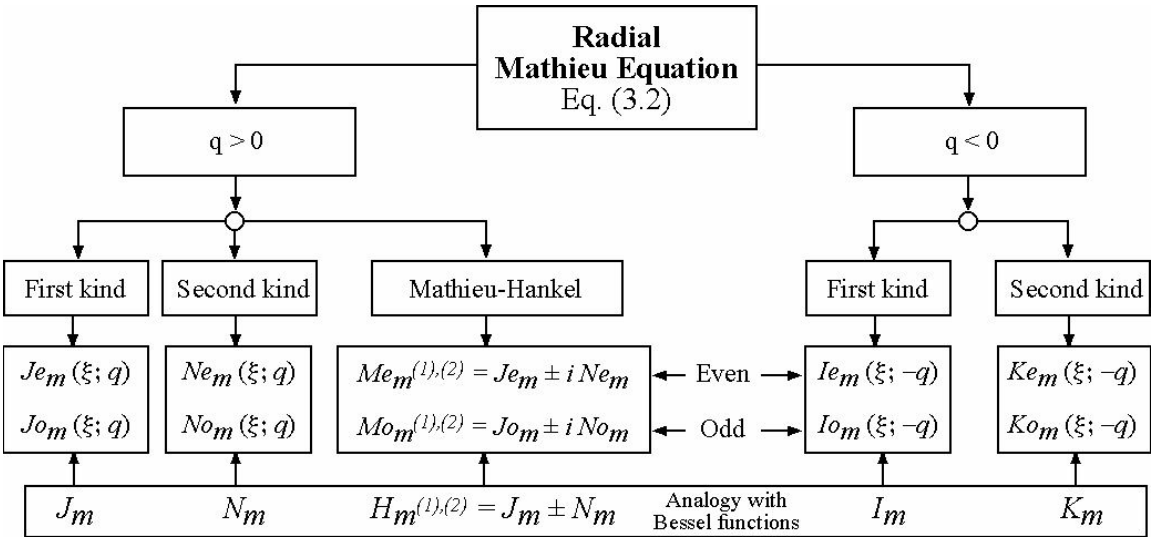


Figure 2-3: Classification of the Radial Mathieu functions.

We can see in diagram (2-3) that each Bessel function has associated two RMFs corresponding to an even and an odd version. The Mathieu solutions with $q > 0$ are related to the solutions of the Ordinary Bessel equation [$J$, and $N$], whereas Mathieu solutions with $q < 0$ are connected with the solutions of the Modified Bessel equation [$I$, and $K$].

Since Bessel functions are well known, visualizing the analogies between them with the RMFs is a very practical way to gain a first understanding of the qualitative behavior of the RMFs. In the next subsections we analyze the procedure to obtain each RMF.

It should be mentioned that there exists other family of Second kind Radial solutions termed $Fe$ and $Ge$. These can be derived from the second kind Angular solutions $fe$ and $ge$ by replacing $\xi$ by $i\xi$. In applications, however, the functions $Ne$ and $No$ are much more convenient than $Fe$ and $Ge$, and this is true quite apart from the slow convergence of the series defining $Fe$ and $Ge$ for large (real) values of $\xi$, and because $Ne$ and $No$ tend to $N$-Bessel function as elliptic coordinates tend to circular coordinates.

### 2.3.1 Case $q > 0$, First kind solutions $Je_m$ and $Jo_m$, [$J$-Bessel type]

Since AME Eq. (2.1) is transformed into RME Eq. (2.2) by writing $\eta$ for $i\xi$, we can derive a set of solutions of the RME by applying this transformation to Eqs. (2.3)-(2.6), namely

$$\text{Class I} \qquad Je_{2n}(\xi;q) = ce_{2n}(i\xi;q) = \sum_{j=0}^{\infty} A_{2j}(q)\cosh(2j\xi)\,, \tag{2.22a}$$

$$\text{Class II} \qquad Je_{2n+1}(\xi;q) = ce_{2n+1}(i\xi;q) = \sum_{j=0}^{\infty} A_{2j+1}(q)\cosh[(2j+1)\xi]\,, \tag{2.22b}$$

$$\text{Class III} \qquad Jo_{2n+2}(\xi;q) = -ise_{2n+2}(i\xi;q) = \sum_{j=0}^{\infty} B_{2j+2}(q)\sinh[(2j+2)\xi]\,, \tag{2.22c}$$

$$\text{Class IV} \qquad Jo_{2n+1}(\xi;q) = -ise_{2n+1}(i\xi;q) = \sum_{j=0}^{\infty} B_{2j+1}(q)\sinh[(2j+1)\xi]\,. \tag{2.22d}$$

Numerically speaking, the rate of convergence of these *hyperbolic* series decreases rapidly with increasing $\xi$, and they are consequently inconvenient for computation, as we will see in Chapter 3. Fortunately, these series can be expressed in terms of summations of *Bessel functions*, or summations of *product of Bessel functions*, which do not have these defects. The series involving Bessel functions converge absolutely and uniformly for all finite values of $\xi$. The rate of convergence of those involving products of Bessel function increases with increasing $\xi$.

For the sake of brevity, we exclusively include in this subsection the representation of the RMF in terms of Bessel function series. The complete list of formulae of the RMF involving the hyperbolic and Bessel function product series is provided in Appendix A. We first define

$$v_1 \equiv \sqrt{q}\exp(-\xi)\,, \qquad \text{and} \qquad v_2 \equiv \sqrt{q}\exp(\xi)\,, \tag{2.23}$$

$$u \equiv v_2 - v_1 = 2\sqrt{q}\sinh\xi, \qquad \text{and} \qquad w \equiv v_1 + v_2 = 2\sqrt{q}\cosh\xi. \tag{2.24}$$

The first kind RMF are written as

$$Je_{2n}(\xi;q) = \frac{ce_{2n}(0,q)}{A_0}\sum_{j=0}^{\infty}A_{2j}J_{2j}(u), \tag{2.25a}$$

$$Je_{2n+1}(\xi;q) = \frac{ce_{2n+1}(0,q)}{\sqrt{q}A_1}\coth(\xi)\sum_{j=0}^{\infty}(2j+1)A_{2j+1}J_{2j+1}(u), \tag{2.25b}$$

$$Jo_{2n+2}(\xi;q) = \frac{se'_{2n+2}(0,q)}{qB_2}\coth(\xi)\sum_{j=0}^{\infty}(2j+2)B_{2j+2}J_{2j+2}(u), \tag{2.25c}$$

$$Jo_{2n+1}(\xi;q) = \frac{se'_{2n+1}(0,q)}{\sqrt{q}B_1}\sum_{j=0}^{\infty}B_{2j+1}J_{2j+1}(u), \tag{2.25d}$$

where the prime denotes the derivative with respect to $\xi$.

Eqs. (2.25) are useful to appreciate the asymptotic behavior of RMFs when the elliptic coordinates tend to circular coordinates. The parameter $q$ is related to the transverse spatial frequency by Eq. (1.13), then $u = k_t f\sinh\xi$. According to the asymptotic behavior of the Fourier coefficients [see Sect. 3.2.5], when $q \to 0$ the coefficients $A_m$ or $B_m$ tends to unity and the others vanish. Therefore $Je_{2n}(\xi;q) \to [ce_{2n}(0,q)/A_0]\,J_{2n}(k_t f\sinh\xi)$, however $f\sinh\xi$ is indeed the $y$-axis which in the circular limit ($\xi$ large) approximates to $f\cosh\xi$ and both can be taken as the radius $\rho$. Finally we have

$$Je_{2n}(\xi;q) \to \frac{ce_{2n}(0,q)}{A_0}J_{2n}(k_t\rho).$$

where the proportionality constant $ce_{2n}(0,q)/A_0$ often is not relevant for applications.

### 2.3.2 Case $q > 0$, Second kind solutions $Ne_m$ and $No_m$, [$N$-Bessel type]

The second kind solutions are obtained by taking advantage of the fact that $J$ and $N$ Bessel functions satisfy the same differential equation and recurrence formulae. We can take the Bessel series representation for the functions $Je$ and $Jo$ Eqs. (2.25), replace therein $J$ by $N$, and transform to Bessel functions product expansions, see Ref. [56]. The results are given by

$$Ne_{2n}(\xi;q) = \frac{p_{2n}}{A_0^2}\sum_{j=0}^{\infty}(-1)^j A_{2j}J_j(v_1)N_j(v_2), \tag{2.26a}$$

$$Ne_{2n+1}(\xi;q) = -\frac{p_{2n+1}}{\sqrt{q}A_1^2}\sum_{j=0}^{\infty}(-1)^j A_{2j+1}\left[J_j(v_1)N_{j+1}(v_2)+J_{j+1}(v_1)N_j(v_2)\right], \tag{2.26b}$$

$$No_{2n+2}(\xi;q) = -\frac{s_{2n+2}}{qB_2^2}\sum_{j=0}^{\infty}(-1)^j B_{2j+2}\left[J_j(v_1)N_{j+2}(v_2)-J_{j+2}(v_1)N_j(v_2)\right], \tag{2.26c}$$

$$No_{2n+1}(\xi;q) = \frac{s_{2n+1}}{\sqrt{q}B_1^2}\sum_{j=0}^{\infty}(-1)^j B_{2j+1}\left[J_j(v_1)N_{j+1}(v_2)-J_{j+1}(v_1)N_j(v_2)\right]. \tag{2.26d}$$

and the cofficients read as

$$p_{2n}(q) \equiv ce_{2n}(0;q)\, ce_{2n}\left(\frac{\pi}{2};q\right), \tag{2.27a}$$

$$p_{2n+1}(q) \equiv ce_{2n+1}(0;q)\, ce'_{2n+1}\left(\frac{\pi}{2};q\right), \tag{2.27b}$$

$$s_{2n+2}(q) \equiv se'_{2n+2}(0;q)\, se'_{2n+2}\left(\frac{\pi}{2};q\right), \tag{2.27c}$$

$$s_{2n+1}(q) \equiv se'_{2n+1}(0;q)\, se_{2n+1}\left(\frac{\pi}{2};q\right), \tag{2.27d}$$

where the prime in $ce'$ and $se'$ denotes the derivative of $ce$ and $se$ with respect to $\xi$.

For computational purposes the series involving Bessel function products are well behaved for all $\mathrm{Re}\,\xi > 0$. For large values of $\mathrm{Re}\,\xi$ the functions $Ne$ and $No$ oscillate in the same manner as the corresponding $Je_m$ or $Jo_m$, with a phase difference of $\pi/2$, [see asymptotic expansions in Sect. 2.5, and typical plots in Chapter 3]

The evaluation of the functions $Ne$ and $No$ when $q < 0$, can be obtained by using the next identities, see Refs. [1, 56].

$$Ne_{2n}(\xi;-q) = (-1)^n Ne_{2n}\left(\xi + i\frac{\pi}{2};q\right), \tag{2.28a}$$

$$Ne_{2n+1}(\xi;-q) = (-1)^{n+1} iNo_{2n+1}\left(\xi + i\frac{\pi}{2};q\right), \tag{2.28b}$$

$$No_{2n+2}(\xi;-q) = (-1)^{n+1} No_{2n+2}\left(\xi + i\frac{\pi}{2};q\right), \tag{2.28c}$$

$$No_{2n+1}(\xi;-q) = (-1)^{n+1} iNe_{2n+1}\left(\xi + i\frac{\pi}{2};q\right). \tag{2.28d}$$

### 2.3.3 Case $q < 0$, First kind solutions $Ie_m$ and $Io_m$, [$I$-Bessel type]

The first kind solutions with $q < 0$ can be obtained by writing $(\xi + i\pi/2)$ for $\xi$ in Eqs. (2.25). After applying the appropriate identities for Bessel functions, the solutions are expressed in terms of $I$-Bessel functions as

$$Ie_{2n}(\xi;-q) = (-1)^n \frac{ce_{2n}(\frac{\pi}{2},q)}{A_0} \sum_{j=0}^{\infty} A_{2j} I_{2j}(u), \tag{2.29a}$$

$$Ie_{2n+1}(\xi;-q) = (-1)^n \frac{se_{2n+1}(\frac{\pi}{2},q)}{\sqrt{q}B_1} \coth\xi \sum_{j=0}^{\infty} (2j+1) B_{2j+1} I_{2j+1}(u), \tag{2.29b}$$

$$Io_{2n+2}(\xi;-q) = (-1)^{n+1} \frac{se'_{2n+2}(\frac{\pi}{2},q)}{qB_2} \coth\xi \sum_{j=0}^{\infty} (2j+2) B_{2j+2} I_{2j+2}(u), \tag{2.29c}$$

$$Io_{2n+1}(\xi;-q) = (-1)^{n+1} \frac{ce'_{2n+1}(\frac{\pi}{2},q)}{\sqrt{q}A_1} \sum_{j=0}^{\infty} A_{2j+1} I_{2j+1}(u). \tag{2.29d}$$

Excepting for the lowest-order function $m = 0$, all first kind solutions with $q < 0$ vanish at $\xi = 0$ and increases monotonically as $\xi$ increases [see typical plots in Chapter 3].

### 2.3.4 Case $q < 0$, Second kind solutions $Ke_m$ and $Ko_m$, [$K$-Bessel type]

These may be obtained from the Bessel function series for $Ne$ and $No$ Eqs. (2.26) by replacing $I_j$ by $(-1)^j K_j$. The factor $1/\pi$ is introduced by McLachlan [56] to systematize the asymptotic relations.

$$Ke_{2n}(\xi;-q) = (-1)^n \frac{p_{2n}}{\pi A_0^2} \sum_{j=0}^{\infty} A_{2j} I_j(v_1) K_j(v_2), \tag{2.30a}$$

$$Ke_{2n+1}(\xi;-q) = (-1)^n \frac{s_{2n+1}}{\pi\sqrt{q} B_1^2} \sum_{j=0}^{\infty} B_{2j+1} \left[ I_j(v_1) K_{j+1}(v_2) - I_{j+1}(v_1) K_j(v_2) \right], \tag{2.30b}$$

$$Ko_{2n+2}(\xi;-q) = (-1)^{n+1} \frac{s_{2n+2}}{\pi q B_2^2} \sum_{j=0}^{\infty} B_{2j+2} \left[ I_j(v_1) K_{j+2}(v_2) - I_{j+2}(v_1) K_j(v_2) \right], \tag{2.30c}$$

$$Ko_{2n+1}(\xi;-q) = (-1)^{n+1} \frac{p_{2n+1}}{\pi\sqrt{q} A_1^2} \sum_{j=0}^{\infty} A_{2j+1} \left[ I_j(v_1) K_{j+1}(v_2) + I_{j+1}(v_1) K_j(v_2) \right]. \tag{2.30d}$$

An important difference between second kind solutions with $q > 0$ [$Ne$ and $No$] with respect to the second kind solutions with $q < 0$ [$Ke$ and $Ko$], is that the former have an oscillatory non-periodic behavior, and the latter have a monotonic decreasing behavior [see typical plots in Chapter 3]. For large $\mathrm{Re}\,\xi$ they tend exponentially to zero, in fact an application of the functions $Ke$ and $Ko$ in Optics is for describing the evanescent fields in the cladding of elliptical dielectric waveguides.

The evaluation of the functions $Ke$ and $Ko$ when $q > 0$ can be obtained by using the following expressions

$$Ke_{2n}(\xi;q) = (-1)^n Ke_{2n}\left(\xi - i\frac{\pi}{2};-q\right), \tag{2.31a}$$

$$Ke_{2n+1}(\xi;q) = (-1)^n Ko_{2n+1}\left(\xi - i\frac{\pi}{2};-q\right), \tag{2.31b}$$

$$Ko_{2n+2}(\xi;q) = (-1)^{n+1} Ko_{2n+2}\left(\xi - i\frac{\pi}{2};-q\right), \tag{2.31c}$$

$$Ko_{2n+1}(\xi;q) = (-1)^n Ke_{2n+1}\left(\xi - i\frac{\pi}{2};-q\right). \tag{2.31d}$$

### 2.3.5 General radial solution of integral order

For $q > 0$, the complete solution of integral order for RME reads as

$$R(\xi) = \sum_{m=0}^{\infty} R_m(\xi) = \sum_{m=0}^{\infty} \begin{cases} A_m Je_m(\xi;q) + B_m Ne_m(\xi;q), & a \in a_m \\ C_{m+1} Jo_{m+1}(\xi;q) + D_{m+1} No_{m+1}(\xi;q), & a \in b_{m+1} \end{cases} \tag{2.32}$$

where $A_m, B_m, C_m$, and $D_m$ are arbitrary constants.

For $q < 0$, the complete solution of integral order for RME is written as

$$R(\xi) = \sum_{m=0}^{\infty} R_m(\xi) = \sum_{m=0}^{\infty} \begin{cases} A_m Ie_m(\xi;-q) + B_m Ke_m(\xi;-q), & a \in a_m \\ C_{m+1} Io_{m+1}(\xi;-q) + D_m Ko_{m+1}(\xi;q), & a \in b_{m+1} \end{cases} \tag{2.33}$$

The numerical behavior of these series, and, in particular, the superiority of the Bessel function product series for computation is demonstrated in the next chapter.

### 2.3.6 Mathieu-Hankel solutions

Analogous to Hankel functions $H_m^{(1),(2)}$ occurring in Bessel equations and circular cylinder coordinates, also exist the Mathieu-Hankel functions of the first and second kind

$$Me_m^{(1)}(\xi;q) = Je_m(\xi;q) + iNe_m(\xi;q), \qquad a \in a_m, \tag{2.34a}$$

$$Me_m^{(2)}(\xi;q) = Je_m(\xi;q) - iNe_m(\xi;q), \qquad a \in a_m, \tag{2.34b}$$

$$Mo_m^{(1)}(\xi;q) = Jo_m(\xi;q) + iNo_m(\xi;q), \qquad a \in b_{m+1}, \tag{2.34c}$$

$$Mo_m^{(2)}(\xi;q) = Jo_m(\xi;q) - iNo_m(\xi;q), \qquad a \in b_{m+1}, \tag{2.34d}$$

As we shall study in Chapter 6, the Mathieu-Hankel functions are used to represent incoming and outgoing waves in problems pertaining to propagating waves. Some authors refer to these functions to as Mathieu functions of the third and fourth kind [1].

### 2.3.7 Asymptotic formulae for large $\xi$

Similar to Bessel functions, the RMFs have useful asymptotic expressions for large $\xi$. These asymptotic formulae can be found with the Bessel function series Eqs. (2.25) and (2.26) by noting that $u$ and $w$ in Eq. (2.24) tend to

$$v_2 = \sqrt{q}\exp(\xi),$$

for large $\xi$. In this section we shall restrict ourselves to list the final results. The asymptotic formulae for the Mathieu-Hankel functions are

$$Me_{2n}^{(1),(2)}(\xi;q) \simeq \frac{p_{2n}}{A_0}\sqrt{\frac{2}{\pi v_2}}\exp\left[\pm i\left(v_2 - \frac{\pi}{4}\right)\right], \tag{2.35a}$$

$$Me_{2n+1}^{(1),(2)}(\xi;q) \simeq -\frac{p_{2n+1}}{\sqrt{q}A_1}\sqrt{\frac{2}{\pi v_2}}\exp\left[\pm i\left(v_2 - \frac{3\pi}{4}\right)\right], \tag{2.35b}$$

$$Mo_{2n+2}^{(1),(2)}(\xi;q) \simeq \frac{s_{2n+2}}{qB_2}\sqrt{\frac{2}{\pi v_2}}\exp\left[\pm i\left(v_2 - \frac{\pi}{4}\right)\right], \tag{2.35c}$$

$$Mo_{2n+1}^{(1),(2)}(\xi;q) \simeq -\frac{s_{2n+1}}{\sqrt{q}B_1}\sqrt{\frac{2}{\pi v_2}}\exp\left[\pm i\left(v_2 - \frac{3\pi}{4}\right)\right], \tag{2.35d}$$

where the constants $p_{2n}$, $p_{2n+1}$, $s_{2n+2}$, and $s_{2n+1}$ are given in Eqs. (2.27). Note that Eq. (2.35a) is a constant multiple of (2.35c), and (2.35b) of (2.35d). Individual expressions for $Je_m$, $Jo_m$, $Ne_m$, and $No_m$ can be deduced directly from Eqs. (2.34)-(2.35).

The asymptotic formulae for RMFs when $q < 0$ are given by

$$\left.\begin{matrix} Ie_{2n}(\xi;-q) \\ Ke_{2n}(\xi;-q) \end{matrix}\right\} \simeq (-1)^n \frac{p_{2n}}{A_0} \frac{\exp(\pm v_2)}{\sqrt{2\pi v_2}}, \tag{2.36a}$$

$$\left.\begin{matrix} Ie_{2n+1}(\xi;-q) \\ Ke_{2n+1}(\xi;-q) \end{matrix}\right\} \simeq (-1)^n \frac{s_{2n+1}}{\sqrt{q}B_1} \frac{\exp(\pm v_2)}{\sqrt{2\pi v_2}}, \tag{2.36b}$$

$$\left.\begin{matrix} Io_{2n+2}(\xi;-q) \\ Ko_{2n+2}(\xi;-q) \end{matrix}\right\} \simeq (-1)^{n+1} \frac{s_{2n+2}}{qB_2} \frac{\exp(\pm v_2)}{\sqrt{2\pi v_2}}, \tag{2.36c}$$

$$\left.\begin{matrix} Io_{2n+1}(\xi;-q) \\ Ko_{2n+1}(\xi;-q) \end{matrix}\right\} \simeq (-1)^{n+1} \frac{p_{2n+1}}{\sqrt{q}A_1} \frac{\exp(\pm v_2)}{\sqrt{2\pi v_2}}. \tag{2.36d}$$

The asymptotic ratio of the functions $Ie_m$ and $Io_m$ is a constant, and each tends to $+\infty$ monotonically as $\xi \to +\infty$.

The asymptotic ratio of the functions $Ke_m$ and $Ko_m$ is a constant, and each tends to $+\infty$ monotonically as $\xi \to +\infty$.

## 2.4 Conclusions

In this Chapter we presented the fundamental theory of the Mathieu equations and the Mathieu functions of integral order. We saw that solving the Angular Mathieu equation leads to solve an eigenvalue problem for the constant of separation $a$. Once found the characteristic values, the Radial Mathieu functions are evaluated with the appropriate expansion series in terms of Bessel functions. Several explicit expressions of these series have been provided. Due to similarities between circular and elliptic coordinates, it is possible to establish strong analogies between the AMFs and the harmonic sine and cosine functions, and between the RMFs with the ordinary and modified Bessel functions. Mathieu-Hankel solutions are an alternative form to present the solutions of the Radial Mathieu equation. This form will be useful in Chapter 5 and 6 to describe travelling waves in elliptic coordinates. Finally we had included some practical asymptotic formulae.

# Chapter 3

# Numerical analysis of the Mathieu functions

With the fundamental theory of the Mathieu differential equations of Chapter 3, now we present a numerical study of the procedures to calculate the characteristic values, the Fourier coefficients, the even and odd AMFs, the even and odd RMFs of first and second kind, and the derivatives of all Mathieu functions.

Since the few efficient algorithms for Mathieu functions which exist are not easily available and the majority of them are limited in range, it was necessary to develop own routines which were appropriate to our specific necessities. In particular the algorithms should be portable, self-contained, and to run efficiently on a conventional 32-bits addressing PC. Besides, they should be called as functions by more general routines. The scope of this chapter is restricted to discuss the Mathieu functions of integer order. The numerical analysis of the functions of fractional order is included in the Appendix B.

This chapter is organized as follows. In Sect. 4.1 we review the numerical literature about the Mathieu functions. The general flowchart is introduced in Sect. 4.2. Computation of the characteristic numbers and the Fourier coefficients is studied in Sects. 4.3 and 4.4 respectively. In Sect. 4.5 we include some convergence tests of our algorithms. The Sect. 4.6 is devoted to show typical plots of several Mathieu functions. Finally Sect. 4.7 are the Conclusions.

## 3.1 Numerical literature review

Following the appearance of E. Mathieu's work [54], some fifty years elapsed before an effective method to calculate the characteristic values was published by E. L. Ince [44]. In that work, Ince solved for the first time the trascendental equations for the characteristic values in the form of infinite continued fractions, and introduced the $(a,q)$-chart for functions of integral order. At the time, due to computational limitations, the results obtained by Ince were restricted to five decimal places for $a_0$, $a_1$, $b_1$, $a_2$, $b_2$, and $q \in [0, 8]$. In 1927 Whittaker and Watson

published the first general study of the theory of Mathieu equations as a chapter of their classical textbook [75], however they did not give a numerical analysis of the evaluation of the solutions.

In 1929, Goldstein provided asymptotic expansions of the characteristics values of the Mathieu equation [29]. On the other hand, many researchers employed the theory of Mathieu functions in multiple applications, [10, **?**, 30, 31, 49, 66, 67], and they improved the basic theory with the finding of new asymptotic formulae and identities. A brief review was presented by Stratton in 1941 [69], and a very extensive treatment with numerical considerations of the Mathieu functions was published by McLachlan in 1947 [56]. G. Blanch [10] outlined in 1946 a method for correcting the characteristic values and the Fourier coefficients based in accurate expressions for the error in the characteristic value computations.

With the advent of the computers, in the early 1960's, some numerical works were published. In 1960, G. Blanch [11] refined the results of Goldstein [29] and Sips [67], by using appropriate expansions in terms of parabolic cylinder functions, and she provided accurate formulae (seven decimal places) for odd periodic Mathieu functions. The characteristic values were recalculated by Blanch in 1964 by using continued fractions [12], and the results were published as a complete chapter in the well-known book by Abramowitz, [1]. The stability of the coefficients and numerical tables for non-periodic Mathieu functions of fractional order were studied by Tamir [71, 72]-. The results of Tamir were refined by H. Früchting in 1969 by evaluating the eigenvalues of a tridiagonal matrix with the help of the bisection method [28].

In 1969, D. Clemm published several pioneering Fortran routines to evaluate the Mathieu functions and their derivatives [15]. To compute the characteristic values, the Clemm's algorithm calculate first a rough approximation based on results from curve-fitting of the available tabulations, and later iterate, using a Newton's method. The Radial Mathieu functions are calculated with Bessel functions product series, and a normalization according to [69] was used. The routines to evaluate the Bessel functions were build-in included in routines for Mathieu functions. The best accuracy reached in the computation of Angular Mathieu functions was $10^{-12}$. The routines are restricted to real positive values of $q$, and $z$. Evidently, the dependence of the routine on the previous tabulations is a disadvantage of the Clemm's algorithm.

W. R. Leeb, in 1979, computed the characteristic values by finding the eigenvalues of a symmetrical tridiagonal matrix [51]. The algorithm provide an accuracy of 9 decimal places for the first 24 characteristic values with $\mathrm{Re}\, q \in [0, 250]$. The Leeb's algorithm is restricted to evaluate only the characteristic numbers, and does not compute the Mathieu functions.

S. R. Rengarajan *et al.,* in 1980, refined the efficiency of Clemm's algorithm by computing the Bessel functions in a separate subroutine [61], and by taking advantage of the normalization scheme defined by McLachlan [56]. The routines have an accuracy of seven decimal places for the first 11 orders of the Angular and Radial Mathieu functions and their derivatives for $q \in [-0.8, 0.8]$. In 1984, Toyama, *et al.,* truncate the continued fractions for characteristic values to twelve components, and they used a regula-falsi method to solve the roots of the resulting polynomials [73]. An accuracy of more than $10^{-9}$ in the range $q \in [0, 30]$ for calculating the first six orders of the Mathieu functions was reported. Unfortunately they did not provide explicit numerical evaluations of the

Mathieu functions.

More recently, in 1993, R. Shirts [65] reported two Fortran routines which calculate the characteristic numbers and Mathieu functions for fractional as well as integer order. The first uses the standard eigenvalue problem of the tridiagonal matrix, whereas, the second employs the usual continued fraction technique to find the characteristic numbers. The routines are optimized to give an accuracy of $10^{-14}$. Shirts provides useful comparative numerical tables for coefficients of the series in case of fractional order. In 1994 A. Lindner *et al.* [52] proposed to evaluate the angular Mathieu functions for integral and fractional order by their modulus and phase. They took advantage of tha independence between the modulus and the characteristic coefficient. The proposed method calculates the modulus of the Mathieu functions and their Wronskian directly without the characteristic exponent.

In 1996, J. J. Stammes *et al* [68] presented a method to calculate the Mathieu functions based on formulating the calculation as an eigenvalue problem. In 1996 F. A. Alhargan [3] provided accurate asymptotic formulae for the computation of the Mathieu characteristic numbers by the introduction of a new normalization scheme.

Finally in 1999, Schneider *et al.,*[63], employed power-series expansions for hyperbolic functions to calculate the Radial Mathieu functions as an alternative to avoid the use of Bessel functions product series. This strategy permits to reduce the computation-time (10 percent average) but the accuracy decreases to five decimal places in the calculation of the zeros of the first kind Radial solutions. Schneider *et al.* do not include the second kind Radial solutions and it is restricted to positive values of $q$, and real values of $z$ only.

We took upon ourselves the job of developing numerical routines based on the theory of the Mathieu functions described in the previous chapter. Our motivation was to look for efficient, accurate, and fast routines which were suitable to be applied in the solution of a wide variety of physical problems involving Mathieu functions. We have developed our programs with MATLAB software, however the numerical analysis provided in this Chapter is generic for any computational language.

## 3.2 General flowchart

In Fig. 3-1 we show our general flowchart for computing the Mathieu functions of Class I, *i.e.* all those functions whose characteristic numbers are $a_{2n}$. The necessary input parameters to evaluate a given Mathieu function or its derivative are the order $m$, the parameter $q$, and the argument $\eta$ or $\xi$. Since the solutions for negative $q$ can be obtained from those for positive $q$, the parameter $q$ is first converted to a positive value. If $q = 0$, then we use appropriated simplifications for this special case.

The subroutine APARES computes the characteristic values $a_{2n}$. The eigenvalues are returned in order of increasing order in an eigenvector array. Next, the subroutine A2N determines the normalized Fourier coefficients $A_{2j}$, and the results are returned in a second vector array. Once determined the coefficients, the appropriate expansion series is selected by depending on the function to evaluate. Finally, after computing the functions for positive $q$, a subroutine is called to perform any needed sign changes if $q$ is negative.

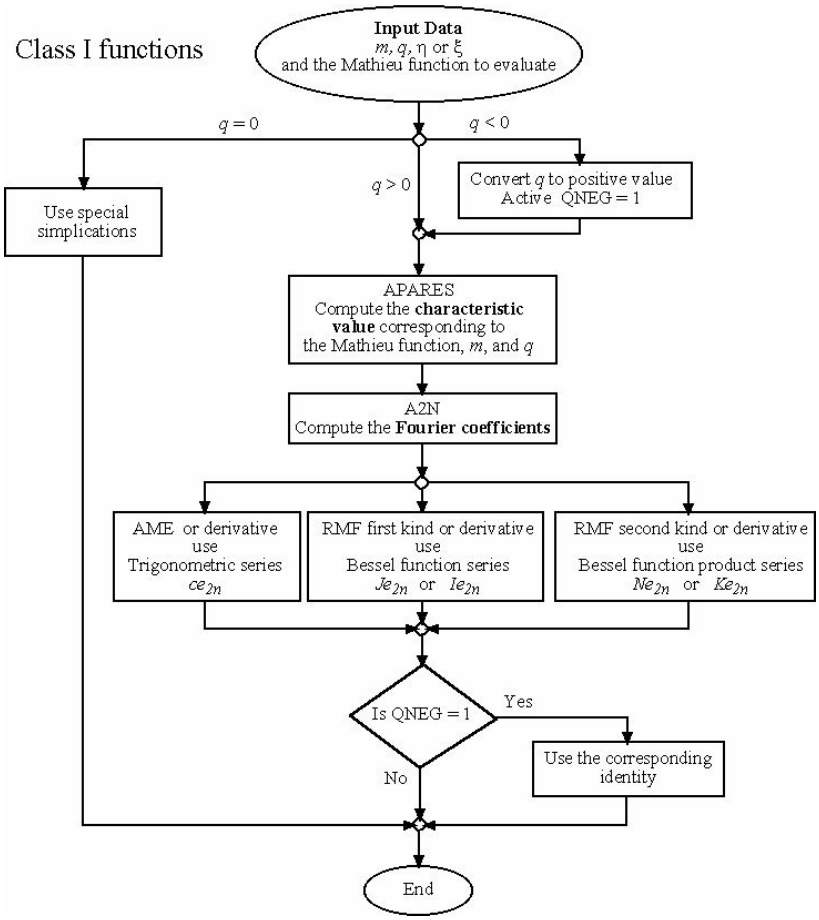


Figure 3-1: General flowchart for computing the Mathieu functions. The subroutine APARES computes the $a_{2n}$ characteristics values. The subroutine A2N compute the $A_{2k}$ coefficintes.

## 3.3 Characteristic values

The characteristic values can be calculated by finding the roots of the continued fractions Eqs. (2.15)-(2.18), or the eigenvalues of the infinite tridiagonal matrix Eq. (C.2) [60]. We have chosen the first method since it is faster, stable, and suitable to be implemented without recursive techniques. Several methods for evaluating continued fractions exist [12, 70], however, the majority of these methods have as objective to evaluate the continued fraction when all elements of the fraction are known *a priori*. In our case, the problem is quite different as the unknown characteristic value $a$ is present in each element of the fraction.

The procedure that we follow to solve Eqs. (2.15)-(2.18) has two steps:

**1.** We first calculate a first approximation for $a$ by truncating the corresponding continued fraction up to 12 elements, next we expand the resulting expression to find a 12-degree polynomial. The roots of this polynomial are the first 12 even or odd characteristic values, as the case may be. The selection of 12 elements was made by using a trial and error method to assure an accuracy of 9 decimal places for $|q| < 40$.

**2.** If an accuracy of more than $10^{-9}$ is desired then a Newton-Cotes higher order method can be used to refine the characteristic value depending on a given tolerance. Nevertheles for the majority of the applications an accuracy of 10-9 is enough..

The subroutine APARES receives as an input parameter the value of $q$. This value is substituted in the continued fraction Eq. (2.15) and the step (1) is applied. An user flag enables the step (2). Finally an eigenvector with the results $[a_0, a_2, ..., a_{22}]$ is returned. The subroutines for calculating the eigenvalues $a_{2n+1}$, $b_{2n+2}$, and $b_{2n+1}$ work in the same manner.

Table 4.1 contains output results from our subroutine BPARES showing an example of the calculation of the characteristic values $b_{2n+2}$. This example uses $q = 25$. In the fourth column we can see that the eigenvalues agree with all significant digits reported by Leeb [51] up 10 figures. Abramowitz [1] reports the two data given in the fifth column where we can see also a total agreement.

**Table 4.1** Example 1: Characteristic numbers $b_{2n+2}$ with $q = 25$

| | BPARES | Leeb | (BPARES-Leeb)/Leeb | Abramowitz |
|---|---|---|---|---|
| $b_2$ | -21.3148606222499 | -21.314860622 | -9.383E-14 | -21.31486062 |
| $b_4$ | 12.9864899527425 | 12.986489953 | -1.982E-11 | not reported |
| $b_6$ | 41.8010712918115 | 41.801071292 | -4.509E-12 | not reported |
| $b_8$ | 69.0579883512758 | 69.057988351 | 3.994E-12 | not reported |
| $b_{10}$ | 103.225680042418 | 103.225680042 | 4.050E-12 | 103.22568004 |
| $b_{12}$ | 146.207674647279 | 146.207674647 | 1.908E-12 | not reported |
| $b_{14}$ | 197.611164920589 | 197.611164916 | 2.322E-11 | not reported |
| $b_{16}$ | 257.22928528627 | 257.229284862 | 1.649E-09 | not reported |

Since the characteristic values are function of $q$, it is possible to construct a $(a, q)$-plane to observe the behavior of the eigenvalues. A chart for the first 6 eigenvalues was shown in Fig. 2-2 in page 12.

## 3.4 Fourier coefficients

Calculating the Fourier coefficients is a more complicated task than the computation of the characteristic values. Since the procedure is recursive, it is necessary to check continuously the convergence of the series. Once computed $a_m$ for a given order $m$ and $q$, the Fourier coefficients are obtained from the recurrence relations Eqs. (2.7)-(2.10). We reproduce the set corresponding to $ce_{2n}$ functions as follows

$$aA_0 - qA_2 = 0, \tag{3.1}$$

$$(a-4)A_2 - q(2A_0 + A_4) = 0, \tag{3.2}$$

$$\left[a - (2j)^2\right] A_{2j} - q(A_{2j-2} + A_{2j+2}) = 0, \qquad j \in \{2, 3, \cdots\} \tag{3.3}$$

Furthermore the coefficients must satisfy the normalization Eq. (2.20). For $ce_{2n}$ we have

$$2A_0^2 + \sum_{j=1}^{\infty} (A_{2j})^2 = 1. \tag{3.4}$$

The typical stable behavior of the coefficients is shown in Fig. 3-2(a). Usually the coefficient $A_m$ has the largest magnitude, although it is not always the case. For $q$ sufficiently large ($q > 30$) the largest coefficient may be $A_{m+2}$ or even $A_{m+4}$. The magnitude of the coefficients decreases, and their signs alternate as $j$ increases.

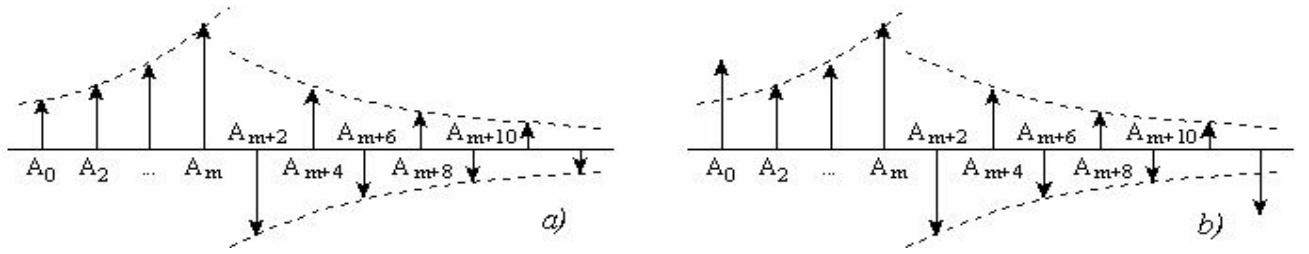


Figure 3-2: *a)* Stable behavior of the Fourier coefficients, and *b)* unstable behavior of the coefficients.

The first alternative to compute the coefficients is referred to as Forward Recurrence Technique (FRT) and it consists on:

1. Suppose an initial value for $A_0$ (*e.g.* $A_0 = 1$),

2. Solve Eq. (3.1) to find $A_2$,

3. Apply Eqs. (3.2)-(3.3) to evaluate the remaining coefficients; the process is interrupted depending on a tolerance for the magnitude of the higher coefficients, and finally

4. The coefficients are rescaled to satisfy normalization.

The convergence problem of FRT appears during the computation of the higher coefficients, specifically when the largest coefficient was already calculated and now the magnitude of the new coefficients is decreasing. To illustrate this problem, let us compute the coefficients for $ce_4$ with $q = 1.5$. By taking a characteristic value $a_4 = 16.077512$, FRT yields the following non-normalized coefficients

$$\begin{aligned} A_0 &= 1, & A_8 &= 0.199122, \\ A_2 &= 10.71834, & A_{10} &= 0.000515, \\ A_4 &= 84.30059, & A_{12} &= -0.227935, \\ A_6 &= -6.36214, & A_{14} &= 19.438117, \end{aligned}$$

It is evident that FRT becomes unstable at $A_{10}$. In Chapter 3, it was demonstrated that the recurrence relations are absolutely convergent. However this convergence is satisfied exclusively if the *exact value* of $a$ is used. Since $a$ is an irrational number, the computer cannot use the exact value, and the FRT has a convergence problem. In other words, the recurrence relations are satisfied if and only if the point $(a, q)$ lies on a characteristic

curve in the $(a, q)$-plane, see Fig. 2-2 in page 12. This instability problem permits us appreciate the importance of calculating the characteristic values with the highest accuracy possible.

A second alternative consists in employing a Backward Recurrence Technique (BRT) instead of FRT. The process starts by using Eq. (2.12) to estimate the coefficient $A_{j\max}$ which may be neglected for a given tolerance (*i.e.*. $A_{j\max} = 0$). Later, suppose an initial value for $A_{j\max-2}$ (*e.g.* $A_{j\max-2} = 1$), and apply the recurrence relation (3.3) to compute $A_{j\max-4}$. The process continues until getting $A_0$. This technique works well for the higher coefficients, however if the order $m$ is sufficiently large, then many coefficients could exist between $A_0$ and the largest coefficient (usually $A_m$), and the algorithm could have convergence problems while it calculates decreasing magnitude coefficients, see Fig. 3-2(b).

In order to minimize the convergence problems discussed above, we implemented an algorithm which combine FRT and BRT, we have termed it Forward and Backward Recurrence Method (FBRM). The $A_{2j}$ coefficients are determined as follows

**1.** With forward recurrence for $2j \in \{0,\ 2,\ 4, ..., m\}$ where $m$ corresponds to the largest coefficient. The result is a vector of non-normalized coefficients. For example, with $m = 6$ we may have $A^+ \equiv [A_0, A_2, A_4, A_6] = [1,$ 23.4, 117.8, 1345.8].

**2.** With backward recurrence for $2j \in \{j\max,\ j\max-2,\ j\max-4, ..., m\}$ where $j\max$ is determined as we explained above. For example $A^- \equiv [A_6, A_8, ..., A_{16}] = [3567.5,$ 1239, 567.5, 124.5, 12.3, 1].

**3.** Since $A_m$ from $A^+$ and $A^-$ must be equal, then $A^-$ is scaled by a factor $A_m^+/A_m^-$, and we now have a complete set of non-normalized coefficients.

**4.** All coefficients are rescaled to satisfy the normalization.

The use of this new algorithm improves notably the results and the stability obtained by FRT and BRT. Table 4.2 illustrates a calculation of coefficients with $m = 10$ and $q = 0.1$. The results show an excellent agreement with Shirts [65]. It is necessary to mention that Shirts's algorithm was designed to calculate fractional order coefficients $c_0, c_2, ...$(including those of integral order $A_0,\ A_2, ...$as a special case). To maintain the values reported by Shirts and to make appropriate comparisons, we convert our integer order results into their fractional order equivalents by using $\sqrt{2}A_0 = c_0$, and $A_j = \sqrt{2}c_j$ for $j \geq 1$. The theory and a brief numerical discussion of fractional order Mathieu functions in included in Appendix B.

**Table 4.2** Example 2: Fourier coefficients with $m = 10$ and $q = 0.1$

| | FRT | BRT | FBRM : A2N | Shirts |
|---|---|---|---|---|
| $c_0$ | 7.61170033181547e-15 | -53.9424062349557 | 7.61170033183669e-15 | 7.61170033178934e-15 |
| $c_2$ | 3.80585208805181e-12 | -1.12380093223648e-01 | 3.80585208806241e-12 | 3.80585208804187e-12 |
| $c_4$ | 3.65361231497444e-09 | -1.33782340078417e-04 | 3.65361231498463e-09 | 3.65361231496803e-09 |
| $c_6$ | 3.06903238398281e-06 | 2.85999102651629e-06 | 3.06903238399136e-06 | 3.06903238398042e-06 |
| $c_8$ | 1.96417862215104e-03 | 1.96417804148689e-03 | 1.96417862215651e-03 | 1.96417862215203e-03 |
| $c_{10}$ | 7.07102226950117e-01 | 7.07102226952087e-01 | 7.07102226952087e-01 | 7.07102226952087e-01 |
| $c_{12}$ | -1.60705674569788e-03 | -1.60705616503272e-03 | -1.60705616503274e-03 | -1.60705616503574e-03 |
| $c_{14}$ | 1.92951317775452e-06 | 1.67401883706807e-06 | 1.67401883706809e-06 | 1.67401883707264e-06 |
| $c_{16}$ | | -1.07308965262173e-09 | -1.07308965262174e-09 | -1.07308965262523e-09 |
| $c_{18}$ | | 4.7905805993572e-13 | 4.79058059935717e-13 | 4.79058059937449e-13 |
| $c_{20}$ | | -1.5968606072335e-16 | -1.59686060723353e-16 | -1.59686060723974e-16 |
| $c_{22}$ | | 4.158491939118e-20 | 4.1584919391182e-20 | 4.15849193913526e-20 |
| $c_{24}$ | | -8.736328848779e-24 | -8.7363288487789e-24 | -8.73632884881624e-24 |
| $c_{26}$ | | | 1.51672389145835e-27 | 1.51672392996215e-27 |

This example shows clearly the convergence problems of BRT. By starting in $c_{24}$ we can see a good agreement between the values of FBRM and Shirts, however, once crossed the largest coefficient $c_{10}$ the instability arises in $c_6$, see Fig. 3-2(b). Note that $c_4$ has an error of $10^5$ with respect the correct value, and this error increases up $10^{16}$ for $c_0$.

## 3.5 Calculating the Mathieu functions based in a matricial method

Besides presenting a visual description of Mathieu functions, it is our intention to provide the scientific and engineering community with a set of subroutines written in Matlab to evaluate them, which we provide in this appendix. The common approach is to compute the eigenvalue $a_m$ for a given order $m$ a value of the $q$ parameter that in applications is given by the problem (see text above). Once this eigenvalue is obtained, we proceed to evaluate the Mathieu functions that generically are of the form $f(m, X, q)$, where $X$ is either the angular or radial variable accordingly.

The first step for the calculation of the Mathieu functions consists on the computation of the characteristic values. There exist different approaches in doing so; the most common method is based on recurrence relations and infinite continued fractions [56, 65]. A second method, the one implemented in this work, consists on reformulating the calculation in an eigenvalue problem [68]. The advantage of the second method is that does not need an initial estimate for the characteristic values, the coefficients are calculated at the same time as the eigenvalues and it is easier to implement into MatLab.

The MatLab functions to compute the characteristic values and the expansion coefficients for the even Mathieu functions of period $\pi$, $ce_{2m}$(z,q), and $2\pi$, $ce_{2m+1}$(z,q), are ***aeven*** and ***aood*** respectively, and for the odd Mathieu functions of period $\pi$, $se_{2m+2}$(z,q), and $2\pi$, $se_{2m+1}$(z,q), are ***beven*** and ***bood*** respectively. They solve the eigenvalue problem to the following matrix systems, for the function $ce_{2m}$(z,q)

$$\begin{bmatrix} -a & \sqrt{2}q & 0 & 0 & 0 & 0 \\ \sqrt{2}q & 2^2-a & q & 0 & 0 & 0 \\ 0 & q & 4^2-a & q & 0 & 0 \\ 0 & 0 & q & 6^2-a & q & 0 \\ 0 & 0 & 0 & q & \vdots & \vdots \\ \vdots & \vdots & \vdots & \vdots & \vdots & \vdots \end{bmatrix} \begin{bmatrix} Ae_0 \\ Ae_2 \\ Ae_4 \\ Ae_6 \\ \vdots \\ \vdots \end{bmatrix} = 0$$

for the function $ce_{2m+1}$(z,q)

$$\begin{bmatrix} 1+q-a & q & 0 & 0 & 0 & 0 \\ q & 3^2-a & q & 0 & 0 & 0 \\ 0 & q & 5^2-a & q & 0 & 0 \\ 0 & 0 & q & 7^2-a & q & 0 \\ 0 & 0 & 0 & q & \vdots & \vdots \\ \vdots & \vdots & \vdots & \vdots & \vdots & \vdots \end{bmatrix} \begin{bmatrix} Ae_1 \\ Ae_3 \\ Ae_5 \\ Ae_7 \\ \vdots \\ \vdots \end{bmatrix} = 0$$

for the functions $se_{2m+2}$(z,q)

$$\begin{bmatrix} 2^2-b & q & 0 & 0 & 0 & 0 \\ q & 4^2-b & q & 0 & 0 & 0 \\ 0 & q & 6^2-b & q & 0 & 0 \\ 0 & 0 & q & 8^2-b & q & 0 \\ 0 & 0 & 0 & q & \vdots & \vdots \\ \vdots & \vdots & \vdots & \vdots & \vdots & \vdots \end{bmatrix} \begin{bmatrix} Be_2 \\ Be_4 \\ Be_6 \\ Be_8 \\ \vdots \\ \vdots \end{bmatrix} = 0$$

and for the function $se_{2m+1}$(z,q)

$$\begin{bmatrix} 1-q-b & q & 0 & 0 & 0 & 0 \\ q & 3^2-b & q & 0 & 0 & 0 \\ 0 & q & 5^2-b & q & 0 & 0 \\ 0 & 0 & q & 7^2-b & q & 0 \\ 0 & 0 & 0 & q & \vdots & \vdots \\ \vdots & \vdots & \vdots & \vdots & \vdots & \vdots \end{bmatrix} \begin{bmatrix} Be_1 \\ Be_3 \\ Be_5 \\ Be_5 \\ \vdots \\ \vdots \end{bmatrix} = 0$$

The second step in the calculation of the Mathieu functions is to compute the infinite series

$$\begin{aligned} ce_{2m}(z,q) &= \sum_{k=0}^{\infty} A_{2k}^{2m}(q)\,\cos(2kz), \\ ce_{2m+1}(z,q) &= \sum_{k=0}^{\infty} A_{2k+1}^{2m+1}(q)\,\cos\left[(2k+1)\,z\right] \\ se_{2m+2}(z,q) &= \sum_{k=0}^{\infty} B_{2k+2}^{2m+2}(q)\,\cos\left[(2k+2)\,z\right] \\ se_{2m+1}(z,q) &= \sum_{k=0}^{\infty} B_{2k+1}^{2m+1}(q)\,\cos\left[(2k+1)\,z\right] \end{aligned}$$

The function ***cem***, computes the $ce_m$(z,q) function, while the function ***sem*** computes the $se_m$(z,q) function for both positive and negative values of q. Although for the majority of the cases a matrix of size 16x16 is enough to get an acceptable accuracy, for certain values of q and m, the size of the matrix has to be increased. So for a given accuracy the size of the matrix increase with the value of q and the order of the Mathieu function.

The Mathieu functions $Je_m$(z,q) and $Jo_m$(z,q), are calculated from the expanded series of Bessel function products [33, 56]. Because the Bessel functions decrease as $k$ increases, a rapid convergence of the series is reached and this is particularly convenient for a wide range of values of q and z. The MatLab functions ***Jem*** and ***Jom*** use these series of Bessel function products and the derivatives of $ce_m$(z,q) and $se_m$(z,q), that are calculated with the functions ***Dcem*** and ***Dsem***.

Finally the calculation of the Mathieu functions $Ne_m$(z,q) and $No_m$(z,q) also uses an expansion series of Bessel function products, and they are calculated in a similar manner as the $Je_m$(z,q) and $Jo_m$(z,q) functions. The MatLab functions ***Nem*** and ***Nom*** implement this algorithm for positive and negative values of the $q$ parameter.

## 3.6 Plots of the Mathieu functions

Once tested our algorithms for discrete values of $\eta$ or $\xi$, in this section we include some typical plots of the Mathieu functions. In Fig. 3-3 we plot the AMFs $ce_m(\eta;q)$ and $se_m(\eta;q)$ for several combinations of $m$ and $q$. The curves with $q = 0$ reduce to the trigonometric functions $\cos(m\eta)$ and $\sin(m\eta)$. For clarity the range in subplots (b) and (d) have been limited to $[0, \pi/2]$, since the whole behavior can be deduced with the symmetry properties of the AMFs. From Fig. 3-3 we can corroborate the next periodicity characteristics

1) The functions $ce_{2n}(\eta;q)$, $n \in \{0, 1, 2.\cdots\}$, have period $\pi$. There is a constant term in the series, which is function of $q$. As a consequence, $ce_0(\eta;q)$ is never negative, although oscillatory.

2) The functions $ce_{2n+1}(\eta;q)$ have period $2\pi$. There is not constant a term in the series.

3) The functions $se_{2n+2}(\eta;q)$ have period $\pi$. There is not constant a term in the series.

4) The functions $se_{2n+1}(\eta;q)$ have period $2\pi$.There is not constant a term in the series.

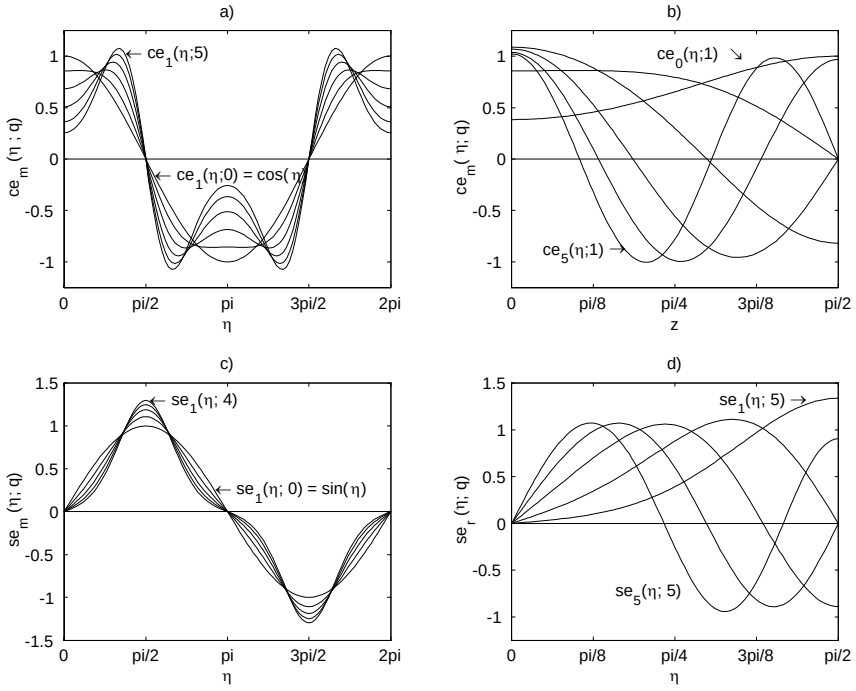


Figure 3-3: Plots of *a)* $ce_m(\eta; q)$, $q = 1$, $m \in \{1, 2, 3, 4, 5\}$ ; *b)* $ce_m(\eta; q)$, $m = 1$, $q \in \{0, 1, 2, 3, 4, 5\}$ ; *c)* $se_m(\eta; q)$, $q = 5$, $m \in \{1, 2, 3, 4, 5\}$ ; *d)* $se_m(\eta; q)$, $m = 1$, $q \in \{0, 1, 2, 3, 4\}$

5) All above functions have $n$ real zeros in the open interval $\eta \in (0, \pi/2)$.

Plots of the lowest-order Radial solutions with $q > 0$ are shown in Fig. 3-4. In subplot 3-4(a) we plot the function $Je_0$ for $q = 1$ (dashed line) and $q = 25$ (solid line). We are plotting $Je_0$ in function of $\sinh(\xi)$ in order to regard the horizontal axis as a normalized $y$-axis, see Eq. (1.1) in page 2. This fact allows us to visualize the behavior of $Je_0$ in function of length units instead of the dimensionless variable $\xi$. Since $q$ is proportional to the squared spatial frequency $k_t$ [Eq. (1.13)], the plot for $q = 25$ oscillates faster than plot for $q = 1$. For large values of $\xi$ the function $Je_0$ exhibits the asymptotic behavior described by Eq. (2.35a), *i.e.* harmonic oscillation with decreasing amplitude as $1/\rho$.

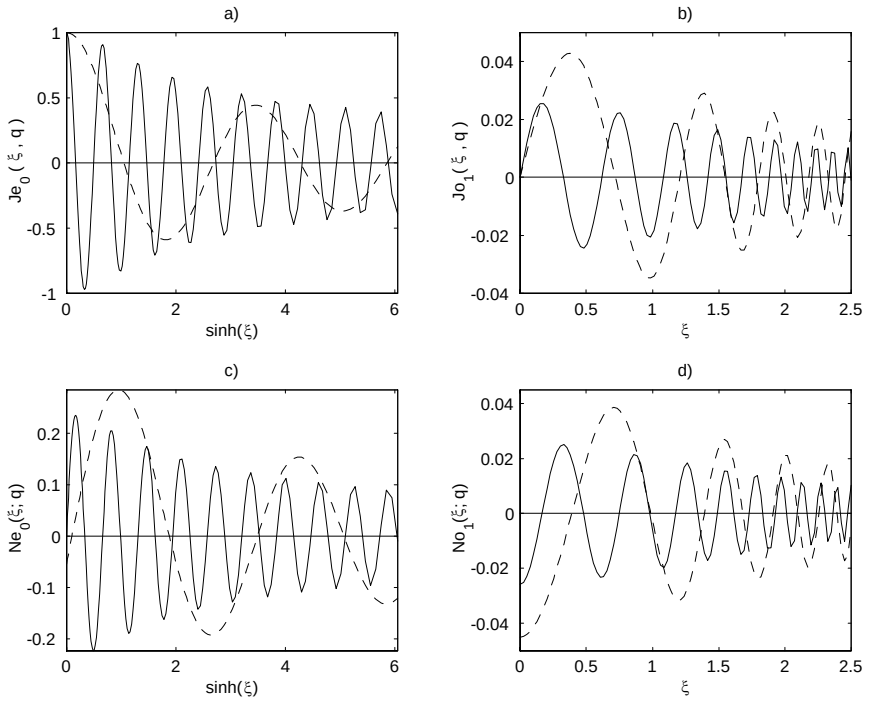


Figure 3-4: Plots of *a)* $Je_0(\xi, q)$, for $q \in \{1, 25\}$, *b)* $Jo_1(\xi, q)$, for $q \in \{5, 25\}$ *c)* $Ne_0(\xi, q)$, for $q \in \{1, 25\}$, *d)* $No_1(\xi, q)$, for $q \in \{5, 25\}$. Continuous lines are for $q = 25$, whereas dashed lines are for $q = 1$ or 5, as the case may be.

The Bessel analogy of $Je_0$ is indeed the lowest-order Bessel function $J_0$. Observe in subplot 3-4(a) that the peak at $\xi = 0$ of $Je_0$ is not as dominant as in case of the $J_0$ function. This fact has interesting physical consequences.

Contrary to $J_0$-Bessel function which has an initial maximum very large compared with respect to the following maxima, the secondary maxima of $Je_0$, although decreasing, have amplitudes similar to that of the initial peak. This fact leads to wave solutions in elliptic coordinates that have a well defined ringed structure. Evidently, for a smaller value of $q$ the initial peak is more dominant.

In Fig. 3-4(b) we show the behavior of $Jo_1$ for $q = 5$ and $q = 25$. In this case we plot as a function of $\xi$ to

compare between plotting in function of $\xi$ or $\sinh\xi$. Whereas in subplot 3-4(a) the oscillations tend to be periodic, in subplot (b) the oscillations get faster as $\xi$ increases. This difference is evidently a result of using different scales in the horizontal axis.

The lowest-order function of second-kind is plotted in Fig. 3-4(c). Note that $Ne_0$ does not indeterminate at $\xi = 0$, as it is the case of the Neumann function $N_0$. It follows that second-kind wave solutions in elliptic coordinates are finite everywhere including the origin.

In Figs. 3-5 and 3-6 we show the behavior of several RMFs for a variety of values of $q$. Subplots 3-5(a,b) allow us to compare the even and odd versions of the first kind RMFs. Note that the slope of even functions always vanish at $\xi = 0$, whereas the odd functions vanish at $\xi = 0$. In subplots 3-5(c,d) we confirm again that Neumann elliptic functions $Ne$ and $No$ are finite at the origin. For smaller values of $q$ the initial values of $Ne$ and $No$ become more negative.

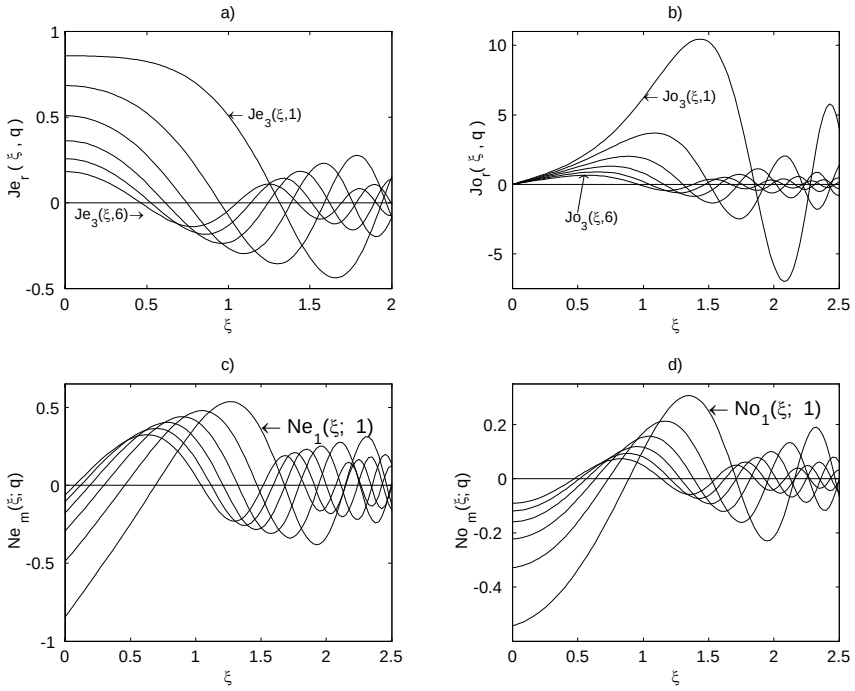


Figure 3-5: Plots of *a)* $Je_3(\xi, q)$, $q \in \{1, 2, .., 6\}$; *b)* $Jo_3(\xi, q)$, $q \in \{1, 2, .., 6\}$; *c)* $Ne_1(\xi, q)$, $q \in \{1, 1.5, 2, 2.5, 3, 3.5\}$; *d)* $No_1(\xi, q)$, $q \in \{1, 1.5, 2, 2.5, 3, 3.5\}$.

The behavior of the RMFs with $q$ negative is shown in Fig. 3-6. Observe that the second kind solutions $Ke$ and $Ko$ in subplots (c) and (d) have finite values at $\xi = 0$. As the parameter $q \to 0$ the initial values $Ke\,(0, q)$ and $Ko\,(0, q)$ tends to infinity.

Finally in Fig.3-7 we show two examples of our algorithms for calculating the derivatives of the first kind solutions.

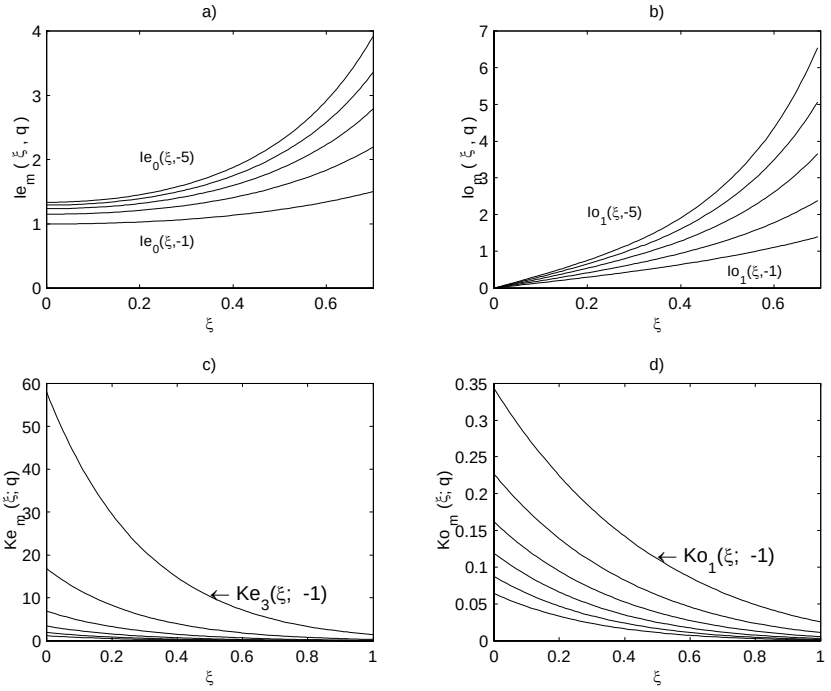


Figure 3-6: Plots of *a)* $Ie_0(\xi,-q)$, $q \in \{1,...,5\}$; *b)* $Io_1(\xi,-q)$, $q \in \{1,...,5\}$; *c)* $Ke_1(\xi,-q)$, $q \in \{1,1.5,2,2.5,3,3.5\}$; *d)* $Ko_1(\xi,-q)$, $m=1$, $q \in \{1,1.5,2,2.5,3,3.5\}$

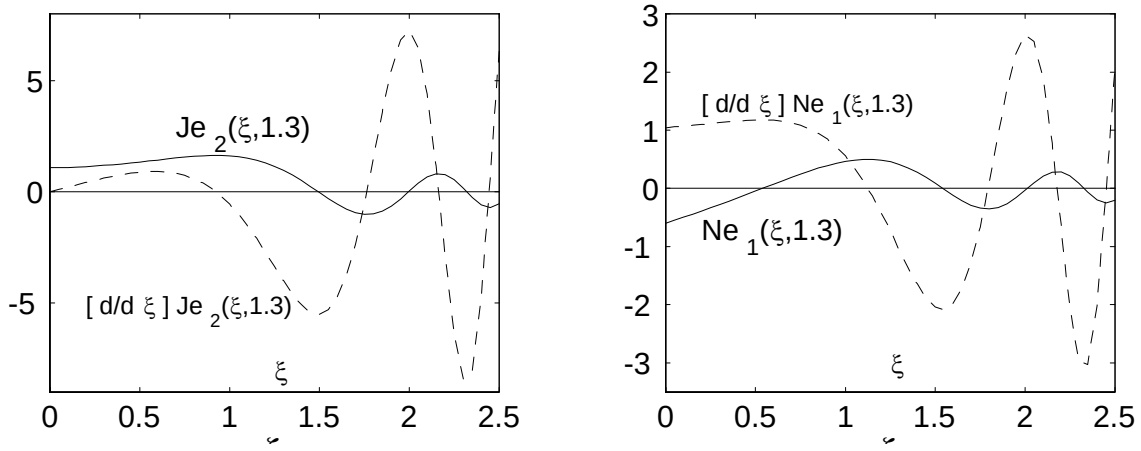


Figure 3-7: Plots of *a)* $Je_2(\xi,1.3)$ and its derivative, *b)* $Ne_1(\xi,1.3)$ and its derivative.

## 3.7 Conclusions

In this Chapter we have presented a numerical method for computing the characteristic values, the Fourier coefficients, and the Angular and Radial Mathieu functions and their derivatives. Based on the tests reported in previos subsections, the general features of our algorithms are listed below

1. Data input: **order** $m \in \{0, 1, ..., 23\}$ ; **parameter** $q \in [-100, 100]$ suggested to maintain below accuracy; **argument** $z$ may be real or complex of unrestricted value. The parameter $q$ and the argument $z$ can be vector arrays .

2. Accuracy of the characteristics values: at least $10^{-9}$.

3. Accuracy of the Fourier coefficients: at least $10^{-7}$.

4. Accuracy of the Mathieu functions: at least $10^{-7}$

The most important conclusions are summarized as follows.

- Calculating the characteristic values by finding the roots of the continued fractions Eqs. (2.15)-(2.18) resulted more efficient than finding the eigenvalues of the infinite tridiagonal matrix Eq. (C.2). Truncation of the continued fractions was convenient to avoid the use of recursive techniques. The method permits to obtain an accuracy of more than $10^{-9}$ in the computation of the characteristics values for the first 23 orders of the Mathieu functions.

- The more efficient method to calculate the Fourier coefficients was a combination of forward and backward recurrence methods. Our algorithm solves the typical convergence problems in the computation of the Fourier coefficients. We noted that usually 16 coefficients are sufficient to assure an accuracy of $10^{-7}$ in the computation of the Mathieu functions. However if this accuracy is not enough, the number of coefficients can be increased by adjusting the tolerance in Eq. (2.12).

- The Bessel function product series presented some advantages over the Bessel series and hyperbolic series in the computation of the RMFs. In particular, the product series converged more rapidly than those with argument $2\sqrt{q}\cosh z$ or $2\sqrt{q}\sinh z$. Besides, the product series for $Ne$, $No$, $Ke$, $Ko$, converged uniformly in any finite region of the $z$-plane, including the origin.

- Using exact expressions for the derivatives of the Mathieu functions resulted in a more accurate, although slower, procedure than any other method based in increments.

# Appendix A

# Identities and miscelaneous relations

The identities between Mathieu functions

$$Ne_{2n}(\xi,q) = iJe_{2n}(\xi,q) - 2Ke_{2n}(\xi,q), \tag{A.1a}$$

$$Ne_{2n}(\xi,-q) = iIe_{2n}(\xi,-q) - 2Ke_{2n}(\xi,-q), \tag{A.1b}$$

$$Ne_{2n+1}(\xi;q) = i\left[Je_{2n+1}(\xi;q) + 2Ke_{2n+1}(\xi;q)\right], \tag{A.1c}$$

$$Ne_{2n+1}(\xi,-q) = iIe_{2n+1}(\xi,-q) + 2Ke_{2n+1}(\xi,-q), \tag{A.1d}$$

$$No_{2n+2}(\xi,q) = iJo_{2n+2}(\xi,q) - 2Ko_{2n+2}(\xi,q), \tag{A.1e}$$

$$No_{2n+2}(\xi,-q) = iIo_{2n+2}(\xi,-q) - 2Ko_{2n+2}(\xi,-q), \tag{A.1f}$$

$$No_{2n+1}(\xi;q) = i\left[Jo_{2n+1}(\xi;q) + 2Ko_{2n+1}(\xi;q)\right], \tag{A.1g}$$

$$No_{2n+1}(\xi,-q) = iIo_{2n+1}(\xi,-q) + 2Ko_{2n+1}(\xi,-q). \tag{A.1h}$$

In Tables 4.3 to 4.5, we show the nature of the Mathieu functions when its argument is real or complex, and $q$ is positive or negative.

**Table 4.3.** Nature of solutions, $\eta$ and $\xi$ are real, and $q > 0$

| | | |
|---|---|---|
| $ce_m(\eta;q) \in$ Re | $Je_m(\xi;q) \in$ Re | $Ne_m(\xi;q) \in$ Re |
| $se_m(\eta;q) \in$ Re | $Jo_m(\xi;q) \in$ Re | $No_m(\xi;q) \in$ Re |
| $fe_m(\eta;q) \in$ Re | $Ie_m(\xi;q) \in$ Re | $Ke_m(\xi;q) \in$ Complex |
| $ge_m(\eta;q) \in$ Re | $Ie_m(\xi;q) \in$ Re | $Ko_m(\xi;q) \in$ Complex |

**Table 4.4.** Nature of the solutions, $\eta$ and $\xi$ are real, and $q < 0$

| | | |
|---|---|---|
| $ce_m(\eta; -q) \in \text{Re}$ | $Je_m(\xi; q) \in \text{Re}$ | $Ne_m(\xi; -q) \in \text{Complex}$ |
| $se_m(\eta; -q) \in \text{Re}$ | $Jo_m(\xi; q) \in \text{Re}$ | $No_m(\xi; -q) \in \text{Complex}$ |
| $fe_m(\eta; -q) \in \text{Re}$ | $Ie_m(\xi; q) \in \text{Re}$ | $Ke_m(\xi; -q) \in \text{Re}$ |
| $ge_m(\eta; -q) \in \text{Re}$ | $Ie_m(\xi; q) \in \text{Re}$ | $Ko_m(\xi; -q) \in \text{Re}$ |

**Table 4.5.** Nature of the solutions, $\eta$ and $\xi$ are purely imaginary

| | | |
|---|---|---|
| $ce_m(\eta; q) \in \text{Re}$ | $Je_m(\xi; \pm q) \in \text{Re}$ | $Ne_m(\xi; \pm q) \in \text{Complex}$ |
| $se_m(\eta; q) \in \text{Im}$ | $Jo_m(\xi; \pm q) \in \text{Im}$ | $No_m(\xi; \pm q) \in \text{Complex}$ |
| $fe_m(\eta; q) \in \text{Im}$ | $Ie_m(\xi; \pm q) \in \text{Re}$ | $Ke_m(\xi; \pm q) \in \text{Complex}$ |
| $ge_m(\eta; q) \in \text{Re}$ | $Io_m(\xi; \pm q) \in \text{Im}$ | $Ko_m(\xi; \pm q) \in \text{Complex}$ |

If arguments $\eta$ and $\xi$ are complex (*i.e.* $\eta = \eta_1 + i\eta_2$) then all functions are complex

Asymptotic expressions of the Radial functions $Ne_m(\xi; q)$, $No_m(\xi; q)$, $Ke_m(\xi, -q)$, and $Ko_m(\xi, -q)$, as $q \to +0$, [56].

$$\left.\begin{matrix} Ne_0(\xi; q) \\ -2Ke_0(\xi, -q) \end{matrix}\right\} \quad \to \quad \frac{\sqrt{2}}{\pi}\left(\xi + \frac{1}{2}\ln q\right), \tag{A.2a}$$

$$\left.\begin{matrix} Ne_m(\xi; q) \\ No_m(\xi; q) \end{matrix}\right\} \quad \to \quad -2^{2m-1}(m-1)!m!\pi^{-1}q^{-m}\exp\left(-m\xi\right), \qquad \text{for } m \geq 1 \tag{A.2b}$$

$$\left.\begin{matrix} Ke_m(\xi, -q) \\ Ko_m(\xi, -q) \end{matrix}\right\} \quad \to \quad -\frac{1}{2}\left\{\begin{matrix} Ne_m(\xi; q) \\ No_m(\xi; q) \end{matrix}\right. , \qquad \text{for } m \geq 1 \tag{A.2c}$$

Derivatives of RMFs and the AMFs and its derivatives

$$Ne'_{2n}(0, q) = \frac{2p_{2n}}{\pi A_0^2} ce_{2n}\left(\frac{\pi}{2}, q\right), \tag{A.3a}$$

$$Ne'_{2n+1}(0, q) = \frac{2p_{2n+1}}{\pi q A_1^2} ce'_{2n+1}\left(\frac{\pi}{2}, q\right), \tag{A.3b}$$

$$No_{2n+2}(0, q) = -\frac{2s_{2n+2}}{\pi q^2 B_2^2} se'_{2n+2}\left(\frac{\pi}{2}, q\right), \tag{A.3c}$$

$$No_{2n+1}(0, q) = -\frac{2s_{2n+1}}{\pi q B_1^2} se_{2n+1}\left(\frac{\pi}{2}, q\right), \tag{A.3d}$$

$$Ke'_{2n}(0,-q) = (-1)^{n+1}\frac{p_{2n}}{\pi A_0^2}ce_{2n}(0,q), \tag{A.4a}$$

$$Ke'_{2n+1}(0,-q) = (-1)^{n+1}\frac{s_{2n+1}}{\pi q B_1^2}se'_{2n+1}(0,q), \tag{A.4b}$$

$$Ko_{2n+2}(0,-q) = (-1)^{n}\frac{s_{2n+2}}{\pi q^2 B_2^2}se'_{2n+2}(0,q), \tag{A.4c}$$

$$Ko_{2n+1}(0,-q) = (-1)^{n}\frac{p_{2n+1}}{\pi q A_1^2}ce_{2n+1}(0,q), \tag{A.4d}$$

# Appendix B

# Detailed procedure to obtain the recurrence relations Eqs. (2.7-3.10)

## B.1 Assuming real solutions procedure

The AME Eq. (2.1) reads as

$$\Theta'' + (a - 2q\cos 2\eta)\,\Theta = 0 \tag{B.5}$$

Due to the periodicity of the solution, we can assume an expansion in terms of Fourier series

$$\Theta(\eta; q) = \sum_{j=0}^{\infty} \left[A_j(q)\cos j\eta + B_{j+1}(q)\sin(j+1)\eta\right].$$

By simplicity, we split the complete solution into an even and an odd solution

$$\Theta(\eta; q) = \Theta_1(\eta; q) + \Theta_2(\eta; q),$$

where $\Theta_1(\eta; q) \equiv ce_m(\eta; q) = \sum_{j=0}^{\infty} A_j(q)\cos j\eta$, and $\Theta_2(\eta; q) \equiv se_{m+1}(\eta; q) = \sum_{j=1}^{\infty} B_j(q)\sin j\eta$.

In order to substitute $\Theta_1(\eta; q)$ into AME, we first obtain the second derivative with respect to $\eta$.

$$\Theta_1''(\eta; q) = -\sum_{j=0}^{\infty} j^2 A_j(q)\cos j\eta$$

Replacing into AME

$$\begin{aligned}\sum_{j=0}^{\infty}\left[(-j^2)A_j\cos j\eta\right]+(a-2q\cos 2\eta)\sum_{j=0}^{\infty}A_j\cos j\eta &= 0\\ \sum_{j=0}^{\infty}\left[(a-j^2)A_j\cos j\eta\right]-2q\cos 2\eta\sum_{j=0}^{\infty}A_j\cos j\eta &= 0\end{aligned}$$

Inserting $\cos 2\eta$ inside the summation, and by using $\cos A\cos B=\frac{1}{2}\left[\cos(A-B)+\cos(A+B)\right]$

$$\begin{aligned}\sum_{j=0}^{\infty}\left[(a-j^2)A_j\cos j\eta\right]-q\sum_{j=0}^{\infty}A_j\left[\cos(j-2)\eta+\cos(j+2)\eta\right] &= 0\\ \sum_{j=0}^{\infty}\left[(a-j^2)A_j\cos j\eta\right]-q\sum_{j=0}^{\infty}A_j\cos(j-2)\eta-q\sum_{j=0}^{\infty}A_j\cos(j+2)\eta &= 0\end{aligned}$$

To make the argument of the cosines equal to $j\eta$, we shift the index of the two final summations.

$$\sum_{j=0}^{\infty}\left[(a-j^2)A_j\cos j\eta\right]-q\sum_{j=-2}^{\infty}A_{j+2}\cos j\eta-q\sum_{j=2}^{\infty}A_{j-2}\cos j\eta=0$$

In order that all summations start at $j=2$, we conveniently extract summands of the first two summations,

$$\begin{aligned}&aA_0+(a-1)A_1\cos\eta+\sum_{j=2}^{\infty}\left[(a-j^2)A_j\cos j\eta\right]\\ &\qquad-\left\{qA_0\cos 2\eta+qA_1\cos\eta+qA_2+qA_3\cos\eta+q\sum_{j=-2}^{\infty}A_{j+2}\cos j\eta\right\}-q\sum_{j=2}^{\infty}A_{j-2}\cos j\eta=0\end{aligned}$$

Due to the presence of the term $qA_0\cos 2\eta$, it is necessary to extract one summand more from the summations.

$$\begin{aligned}&(aA_0-qA_2)+\left[(a-1)A_1-q(A_1+A_3)\right]\cos\eta\\ &\qquad\left[(a-4)\,A_2-q(2A_0+A_4)\right]\cos 2\eta+\sum_{j=3}^{\infty}\left[(a-j^2)A_j-(A_{j+2}+A_{j-2})\right]\cos j\eta=0\end{aligned}$$

where $\cos j\eta$ has been factorized. Since the above equation must be satisfied for any $\eta$, then the multipliers of the cosines must vanish. It is evident from coefficients, that recurrence relations involve only even indexes or odd indexes, yielding two families of recurrence relations.

For even coefficients

$$\begin{aligned}aA_0-qA_2 &= 0,\\ (a-4)\,A_2-q(2A_0+A_4) &= 0,\\ (a-j^2)A_j-(A_{j+2}+A_{j-2}) &= 0,\qquad j\in\{4,6,8,\cdots\}\end{aligned}$$

For odd coefficients

$$\begin{aligned}(a-1)A_1 - q(A_1+A_3) &= 0,\\ (a-j^2)A_j - (A_{j+2}+A_{j-2}) &= 0, \qquad j\in\{3,5,7,\cdots\}\end{aligned}$$

By starting in the same form with the second solution $\Theta_2(\eta;q)$, we can arrive to recurrence relations Eqs. (2.9)-(2.10).

## B.2 Assuming complex solutions procedure

It is interesting to compare the before procedure if we suppose a complex-form solution. The next analysis is more general because it applies to fractional order functions $\beta\in(0,1)$, as well as integral order $\beta\in\{0,1\}$.

By using $\cos 2\eta = [\exp(i2\eta)+\exp(-i2\eta)]/2$, we express the AME in complex form

$$\Theta'' + \{a - q[\exp(i2\eta)+\exp(-i2\eta)]\}\Theta = 0. \tag{B.6}$$

We assume a general solution of the form

$$\Theta(\eta) = \Theta_1(\eta)+\Theta_2(\eta) = e^{i\beta\eta}\sum_{j=-\infty}^{\infty} c_j e^{ij\eta} + e^{-i\beta\eta}\sum_{j=-\infty}^{\infty} c_j e^{-ij\eta},$$

where $c_j\in$ Re are the unknown coefficients.

Derivating $\Theta_1(\eta)$ twice, we get $\Theta_1''(\eta) = -\sum_{j=-\infty}^{\infty}(j+\beta)^2 c_j e^{i(j+\beta)\eta}$, which is inserted in AME Eq. B.6 to obtain

$$\begin{aligned}-\sum_{j=-\infty}^{\infty}(j+\beta)^2 c_j e^{i(j+\beta)\eta} + \left[a - q\left(e^{i2\eta}+e^{-i2\eta}\right)\right]\sum_{j=-\infty}^{\infty} c_j e^{i(j+\beta)\eta} &= 0,\\ \sum_{j=-\infty}^{\infty}\left[a-(j+\beta)^2\right]c_j e^{i(j+\beta)\eta} - q\sum_{j=-\infty}^{\infty}\left[c_j e^{i(j+2+\beta)\eta} + c_j e^{i(j-2+\beta)\eta}\right] &= 0.\end{aligned}$$

To factorize the exponential term, we shift the index of the last two summations

$$\begin{aligned}\sum_{j=-\infty}^{\infty}\left[a-(j+\beta)^2\right]c_j e^{i(j+\beta)\eta} - q\sum_{j=-\infty}^{\infty}\left[c_{j-2}e^{i(j+\beta)\eta} + c_{j+2}e^{i(j+\beta)\eta}\right] &= 0,\\ \sum_{j=-\infty}^{\infty}\left\{\left[a-(j+\beta)^2\right]c_j - q(c_{j-2}+c_{j+2})\right\}e^{i(j+\beta)\eta} &= 0.\end{aligned}$$

where it is clear that fractional coefficients must satisfy the following recurrence relation

$$\left[a-(j+\beta)^2\right]c_j - q(c_{j-2}+c_{j+2}) = 0, \qquad j\in\{\cdots,-2,-1,0,1,2,\cdots\}. \tag{B.7}$$

# Appendix C

# Matrix formulation for the characteristic values $a_{2n}$

The recurrence relations Eqs. (2.7)

$$\begin{aligned} aA_0 - qA_2 &= 0, \\ (a-4)\,A_2 - q(2A_0 + A_4) &= 0, \\ \left[a-(2j)^2\right] A_{2j} - q(A_{2j-2} + A_{2j+2}) &= 0, \qquad j \in \{2,3,...\} \end{aligned}$$

form an infinite set of linear equations, whose unknown coefficients are the Fourier coefficients of the expansions for the Mathieu functions of integral order.

If we use $W_j \equiv -1/V_j = -q/\left(a-j^2\right)$, above equations become

$$\begin{aligned} A_0 + W_0 A_2 &= 0, \\ 2W_2 A_0 + A_2 + W_2 A_4 &= 0, \\ W_{2j} A_{2j-2} + A_{2j} + W_{2j} A_{2j+2} &= 0, \qquad j \in \{2,3,...\} \end{aligned}$$

By writing explicitly the first equations of the set we obtain

$$\begin{array}{ccccccccc} A_0 & +W_0A_2 & & & & & \cdots & = 0 \\ 2W_2A_0 & +A_2 & +W_2A_4 & & & & \cdots & = 0 \\ & W_4A_2 & +A_4 & +W_4A_6 & & & \cdots & = 0 \\ & & W_6A_4 & +A_6 & W_6A_8 & & \cdots & = 0 \\ & & & W_8A_6 & +A_8 & W_8A_{10} & \cdots & = 0 \\ \vdots & \vdots & \vdots & \vdots & \vdots & \vdots & \ddots & ... \end{array} \tag{C.1}$$

A non-trivial solution to this linear set exist only if the determinant of the corresponding matrix vanish

$$D(a,q) \equiv \begin{bmatrix} 1 & W_0 & 0 & 0 & 0 & 0 & \cdots \\ 2W_2 & 1 & W_2 & 0 & 0 & 0 & \cdots \\ 0 & W_4 & 1 & W_4 & 0 & 0 & \cdots \\ 0 & 0 & W_6 & 1 & W_6 & 0 & \cdots \\ 0 & 0 & 0 & W_8 & 1 & W_8 & \cdots \\ \vdots & \vdots & \vdots & \ddots & \vdots & \vdots & \ddots \end{bmatrix} \equiv 0 \tag{C.2}$$

Since $q$ is known, Eq. (C.2) constitutes an equation for $a$. With respect to the convergence of Eq. (C.2), an infinite determinant is absolutely convergent if *a)* the product of the diagonal elements is absolutely convergent, and *b)* the sum of the non-diagonal elements is absolutely convergent. *(a)* is satisfied, since the product is unity, while for *(b)* it is clear that $\sum_{j=0}^{\infty} W_{2j} = \sum_{j=0}^{\infty} q/\left(4j^2 - a\right)$, is convergent since $q/\left(4j^2 - a\right) \to 0$ as $j \to \infty$.

The determinant equations for the remaining characteristic values $a_{2n+1}$, $b_{2n+2}$ and $b_{2n+1}$ can be obtained by following a similar procedure.

# Appendix D

# Formulae for Radial Mathieu functions

In this section we provide a complete list of formulae and identities for calculating the Radial Mathieu functions. We first define some abbreviations used in the expressions.

$$v_1 \equiv \sqrt{q}\exp(-\xi), \qquad \text{and} \qquad v_2 \equiv \sqrt{q}\exp(\xi), \tag{D.1a}$$

$$u \equiv v_2 - v_1 = 2\sqrt{q}\sinh\xi, \qquad \text{and} \qquad w \equiv v_1 + v_2 = 2\sqrt{q}\cosh\xi, \tag{D.1b}$$

$$p_{2n} \equiv ce_{2n}(0,q)\, ce_{2n}\left(\frac{\pi}{2};q\right), \tag{D.2a}$$

$$p_{2n+1} \equiv ce_{2n+1}(0,q)\, ce'_{2n+1}\left(\frac{\pi}{2};q\right), \tag{D.2b}$$

$$s_{2n+2} \equiv se'_{2n+2}(0,q)\, se'_{2n+2}\left(\frac{\pi}{2};q\right), \tag{D.2c}$$

$$s_{2n+1} \equiv se'_{2n+1}(0,q)\, se_{2n+1}\left(\frac{\pi}{2};q\right), \tag{D.2d}$$

In general, there are four types of expansions for each RMF: hyperbolic series, Bessel function series with argument $u$, Bessel function series with argument $w$, and Bessel function product series.

## D.1 First kind solutions $Je_m$ and $Jo_m$, case $q > 0$, [$J$-Bessel type]

The RMFs of the first kind are obtained by replacing $\eta$ by $i\xi$ in trigonometric series for the Angular Mathieu functions Eqs. (2.7)-(2.10). The explicit expression for the four types of expansions are

$$
\begin{aligned}
Je_{2n}(\xi;q) &= ce_{2n}(i\xi;q) = \sum_{j=0}^{\infty} A_{2j}(q)\cosh(2j\xi)\,, && \text{(D.3a)}\\
&= \frac{ce_{2n}(0,q)}{A_0}\sum_{j=0}^{\infty} A_{2j}J_{2j}(u), && \text{(D.3b)}\\
&= \frac{ce_{2n}(\frac{\pi}{2},q)}{A_0}\sum_{j=0}^{\infty}(-1)^j A_{2j}J_{2j}(w), && \text{(D.3c)}\\
&= \frac{p_{2n}}{A_0^2}\sum_{j=0}^{\infty}(-1)^j A_{2j}J_j(v_1)J_j(v_2), && \text{(D.3d)}\\
Je_{2n+1}(\xi;q) &= ce_{2n+1}(i\xi;q) = \sum_{j=0}^{\infty} A_{2j+1}(q)\cosh[(2j+1)\xi]\,, && \text{(D.3e)}\\
&= \frac{ce_{2n+1}(0,q)}{\sqrt{q}A_1}\coth\xi\sum_{j=0}^{\infty}(2j+1)A_{2j+1}J_{2j+1}(u), && \text{(D.3f)}\\
&= -\frac{ce'_{2n+1}(\frac{\pi}{2},q)}{\sqrt{q}A_1}\sum_{j=0}^{\infty}(-1)^j A_{2j+1}J_{2j+1}(w), && \text{(D.3g)}\\
&= -\frac{p_{2n+1}}{\sqrt{q}A_1^2}\sum_{j=0}^{\infty}(-1)^j A_{2j+1}\left[J_j(v_1)J_{j+1}(v_2)+J_{j+1}(v_1)J_j(v_2)\right], && \text{(D.3h)}\\
Jo_{2n+2}(\xi;q) &= -ise_{2n+2}(i\xi;q) = \sum_{j=0}^{\infty} B_{2j+2}(q)\sinh[(2j+2)\xi]\,, && \text{(D.3i)}\\
&= \frac{se'_{2n+2}(0,q)}{qB_2}\coth\xi\sum_{j=0}^{\infty}(2j+2)B_{2j+2}J_{2j+2}(u), && \text{(D.3j)}\\
&= -\frac{se'_{2n+2}(\frac{\pi}{2},q)}{qB_2}\tanh\xi\sum_{j=0}^{\infty}(-1)^j(2j+2)B_{2j+2}J_{2j+2}(w), && \text{(D.3k)}\\
&= -\frac{s_{2n+2}}{qB_2^2}\sum_{j=0}^{\infty}(-1)^j B_{2j+2}\left[J_j(v_1)J_{j+2}(v_2)-J_{j+2}(v_1)J_j(v_2)\right], && \text{(D.3l)}\\
Jo_{2n+1}(\xi;q) &= -ise_{2n+1}(i\xi;q) = \sum_{j=0}^{\infty} B_{2j+1}(q)\sinh[(2j+1)\xi]\,, && \text{(D.3m)}\\
&= \frac{se'_{2n+1}(0,q)}{\sqrt{q}B_1}\sum_{j=0}^{\infty} B_{2j+1}J_{2j+1}(u), && \text{(D.3n)}\\
&= \frac{se_{2n+1}(\frac{\pi}{2},q)}{\sqrt{q}B_1}\tanh\xi\sum_{j=0}^{\infty}(-1)^j(2j+1)B_{2j+1}J_{2j+1}(w), && \text{(D.3o)}\\
&= \frac{s_{2n+1}}{\sqrt{q}B_1^2}\sum_{j=0}^{\infty}(-1)^j B_{2j+1}\left[J_j(v_1)J_{j+1}(v_2)-J_{j+1}(v_1)J_j(v_2)\right], && \text{(D.3p)}
\end{aligned}
$$

## D.2 Second kind solutions $Ne_m$ and $No_m$, case $q > 0$, [$N$-Bessel type]

The series involving functions with arguments $\cosh z$ (*i.e.* symbol $\star$) or $\sinh z$ (*i.e.* symbol ‡) converge non-uniformly as $|\cosh z| \to 1$ or $|\sinh z| \to 1$. For computational purposes the series involving Bessel function products are well behaved for all $\operatorname{Re} z > 0$.

$$
\begin{aligned}
Ne_{2n}(z;q) &= \frac{ce_{2n}(0,q)}{A_0}\sum_{j=0}^{\infty} A_{2j}N_{2j}(u), \qquad ‡ && \text{(D.4a)}\\
&= \frac{ce_{2n}(\frac{\pi}{2},q)}{A_0}\sum_{j=0}^{\infty}(-1)^j A_{2j}N_{2j}(w), \qquad \star && \text{(D.4b)}\\
&= \frac{p_{2n}}{A_0^2}\sum_{j=0}^{\infty}(-1)^j A_{2j}J_j(v_1)N_j(v_2) && \text{(D.4c)}\\
Ne_{2n+1}(z;q) &= \frac{ce_{2n+1}(0,q)}{\sqrt{q}A_1}\coth z\sum_{j=0}^{\infty}(2j+1)A_{2j+1}N_{2j+1}(u), \qquad ‡ && \text{(D.4d)}\\
&= -\frac{ce'_{2n+1}(\frac{\pi}{2},q)}{\sqrt{q}A_1}\sum_{j=0}^{\infty}(-1)^j A_{2j+1}N_{2j+1}(w), \qquad \star && \text{(D.4e)}\\
&= -\frac{p_{2n+1}}{\sqrt{q}A_1^2}\sum_{j=0}^{\infty}(-1)^j A_{2j+1}\left[J_j(v_1)N_{j+1}(v_2)+J_{j+1}(v_1)N_j(v_2)\right] && \text{(D.4f)}\\
No_{2n+2}(z;q) &= \frac{se'_{2n+2}(0,q)}{qB_2}\coth z\sum_{j=0}^{\infty}(2j+2)B_{2j+2}N_{2j+2}(u), \qquad ‡ && \text{(D.4g)}\\
&= -\frac{se'_{2n+2}(\frac{\pi}{2},q)}{qB_2}\tanh z\sum_{j=0}^{\infty}(-1)^j(2j+2)B_{2j+2}N_{2j+2}(w), \qquad \star && \text{(D.4h)}\\
&= -\frac{s_{2n+2}}{qB_2^2}\sum_{j=0}^{\infty}(-1)^j B_{2j+2}\left[J_j(v_1)N_{j+2}(v_2)-J_{j+2}(v_1)N_j(v_2)\right] && \text{(D.4i)}\\
No_{2n+1}(z;q) &= \frac{se'_{2n+1}(0,q)}{\sqrt{q}B_1}\sum_{j=0}^{\infty}B_{2j+1}N_{2j+1}(u), \qquad ‡ && \text{(D.4j)}\\
&= \frac{se_{2n+1}(\frac{\pi}{2},q)}{\sqrt{q}B_1}\tanh z\sum_{j=0}^{\infty}(-1)^j(2j+1)B_{2j+1}N_{2j+1}(w), \qquad \star && \text{(D.4k)}\\
&= \frac{s_{2n+1}}{\sqrt{q}B_1^2}\sum_{j=0}^{\infty}(-1)^j B_{2j+1}\left[J_j(v_1)N_{j+1}(v_2)-J_{j+1}(v_1)N_j(v_2)\right] && \text{(D.4l)}
\end{aligned}
$$

## D.3 First kind solutions $Ie_m$ and $Ie_m$, case $q<0$, [ $I$-Bessel type]

These solutions are obtained by writing $(\xi + i\pi/2)$ for $\xi$ in Eqs. (D.3a)-(D.3p).

$$Ie_{2n}(\xi,-q) = (-1)^n Je_{2n}(\xi+i\frac{\pi}{2},q) = (-1)^n\sum_{j=0}^{\infty}(-1)^j A_{2j}\cosh(2j\xi), \tag{D.5a}$$

$$= (-1)^n\frac{ce_{2n}(\frac{\pi}{2},q)}{A_0}\sum_{j=0}^{\infty}A_{2j}I_{2j}(u), \tag{D.5b}$$

$$= (-1)^n\frac{ce_{2n}(0,q)}{A_0}\sum_{j=0}^{\infty}(-1)^j A_{2j}I_{2j}(w), \tag{D.5c}$$

$$= (-1)^n\frac{p_{2n}}{A_0^2}\sum_{j=0}^{\infty}(-1)^j A_{2j}I_j(v_1)I_j(v_2), \tag{D.5d}$$

$$Ie_{2n+1}(\xi,-q) = (-1)^{n+1} iJo_{2n+1}(\xi+i\frac{\pi}{2},q) = (-1)^n\sum_{j=0}^{\infty}(-1)^j B_{2j+1}\cosh[(2j+1)\xi], \tag{D.5e}$$

$$= (-1)^n\frac{se_{2n+1}(\frac{\pi}{2},q)}{\sqrt{q}B_1}\coth\xi\sum_{j=0}^{\infty}(2j+1)B_{2j+1}I_{2j+1}(u), \tag{D.5f}$$

$$= (-1)^n\frac{se'_{2n+1}(0,q)}{\sqrt{q}B_1}\sum_{j=0}^{\infty}(-1)^j B_{2j+1}I_{2j+1}(w), \tag{D.5g}$$

$$= (-1)^n\frac{s_{2n+1}}{\sqrt{q}B_1^2}\sum_{j=0}^{\infty}(-1)^j B_{2j+1}[I_j(v_1)I_{j+1}(v_2)+I_{j+1}(v_1)I_j(v_2)], \tag{D.5h}$$

$$Io_{2n+2}(\xi,-q) = (-1)^{n+1} Jo_{2n+2}(\xi+i\frac{\pi}{2},q) = (-1)^n\sum_{j=0}^{\infty}(-1)^j B_{2j+2}\sinh[(2j+2)\xi], \tag{D.5i}$$

$$= (-1)^{n+1}\frac{se'_{2n+2}(\frac{\pi}{2},q)}{qB_2}\coth\xi\sum_{j=0}^{\infty}(2j+2)B_{2j+2}I_{2j+2}(u), \tag{D.5j}$$

$$= (-1)^n\frac{se'_{2n+2}(0,q)}{qB_2}\tanh\xi\sum_{j=0}^{\infty}(-1)^j(2j+2)B_{2j+2}I_{2j+2}(w), \tag{D.5k}$$

$$= (-1)^{n+1}\frac{s_{2n+2}}{qB_2^2}\sum_{j=0}^{\infty}(-1)^j B_{2j+2}[I_j(v_1)I_{j+2}(v_2)-I_{j+2}(v_1)I_j(v_2)], \tag{D.5l}$$

$$Io_{2n+1}(\xi,-q) = (-1)^{n+1} iJe_{2n+1}(\xi+i\frac{\pi}{2},q) = (-1)^n\sum_{j=0}^{\infty}(-1)^j A_{2j+1}\sinh[(2j+1)\xi], \tag{D.5m}$$

$$= (-1)^{n+1}\frac{ce'_{2n+1}(\frac{\pi}{2},q)}{\sqrt{q}A_1}\sum_{j=0}^{\infty}A_{2j+1}I_{2j+1}(u), \tag{D.5n}$$

$$= (-1)^n\frac{ce_{2n+1}(0,q)}{\sqrt{q}A_1}\tanh\xi\sum_{j=0}^{\infty}(-1)^j(2j+1)A_{2j+1}I_{2j+1}(w), \tag{D.5o}$$

$$= (-1)^n\frac{p_{2n+1}}{\sqrt{q}A_1^2}\sum_{j=0}^{\infty}(-1)^j A_{2j+1}[I_j(v_1)I_{j+1}(v_2)-I_{j+1}(v_1)I_j(v_2)], \tag{D.5p}$$

## D.4 Second kind solutions $Ke_m$ and $Ko_m$, case $q < 0$, [ $K$-Bessel type]

These may be obtained from the Bessel function series in Eqs. (D.5a)-(D.5p) by replacing $I_j$ by $(-1)^j K_j$.

$$
\begin{aligned}
Ke_{2n}(\xi,-q) &= (-1)^n Ke_{2n}(\xi, q+i\frac{\pi}{2}) && \text{(D.6a)}\\
&= (-1)^n \frac{ce_{2n}(\frac{\pi}{2},q)}{\pi A_0}\sum_{j=0}^{\infty} A_{2j}K_{2j}(u), \quad \ddagger && \text{(D.6b)}\\
&= (-1)^n \frac{ce_{2n}(0,q)}{\pi A_0}\sum_{j=0}^{\infty}(-1)^j A_{2j}K_{2j}(w), \quad \star && \text{(D.6c)}\\
&= (-1)^n \frac{p_{2n}}{\pi A_0^2}\sum_{j=0}^{\infty} A_{2j}I_j(v_1)K_j(v_2) && \text{(D.6d)}\\
Ke_{2n+1}(\xi,-q) &= (-1)^n Ko_{2n+1}(z, q+i\frac{\pi}{2}) && \text{(D.6e)}\\
&= \frac{se_{2n+1}(\frac{\pi}{2},q)}{\pi\sqrt{q}B_1}\coth\xi\sum_{j=0}^{\infty}(2j+1)B_{2j+1}K_{2j+1}(u), \quad \ddagger && \text{(D.6f)}\\
&= (-1)^n \frac{se'_{2n+1}(0,q)}{\pi\sqrt{q}B_1}\sum_{j=0}^{\infty}(-1)^j B_{2j+1}K_{2j+1}(w), \quad \star && \text{(D.6g)}\\
&= (-1)^n \frac{s_{2n+1}}{\pi\sqrt{q}B_1^2}\sum_{j=0}^{\infty} B_{2j+1}\left[I_j(v_1)K_{j+1}(v_2) - I_{j+1}(v_1)K_j(v_2)\right] && \text{(D.6h)}\\
Ko_{2n+2}(\xi,-q) &= (-1)^{n+1} Ko_{2n+2}(z, q+i\frac{\pi}{2}) && \text{(D.6i)}\\
&= (-1)^{n+1}\frac{se'_{2n+2}(\frac{\pi}{2},q)}{\pi q B_2}\coth\xi\sum_{j=0}^{\infty}(2j+2)B_{2j+2}K_{2j+2}(u), \quad \ddagger && \text{(D.6j)}\\
&= (-1)^n \frac{se'_{2n+2}(0,q)}{\pi q B_2}\tanh\xi\sum_{j=0}^{\infty}(-1)^j(2j+2)B_{2j+2}K_{2j+2}(w), \quad \star && \text{(D.6k)}\\
&= (-1)^{n+1}\frac{s_{2n+2}}{\pi q B_2^2}\sum_{j=0}^{\infty} B_{2j+2}\left[I_j(v_1)K_{j+2}(v_2) - I_{j+2}(v_1)K_j(v_2)\right] && \text{(D.6l)}\\
Ko_{2n+1}(\xi,-q) &= (-1)^n Ke_{2n+1}(z, q+i\frac{\pi}{2}) && \text{(D.6m)}\\
&= (-1)^{n+1}\frac{ce'_{2n+1}(\frac{\pi}{2},q)}{\pi\sqrt{q}A_1}\sum_{j=0}^{\infty} A_{2j+1}K_{2j+1}(u), \quad \ddagger && \text{(D.6n)}\\
&= (-1)^n \frac{ce_{2n+1}(0,q)}{\pi\sqrt{q}A_1}\tanh\xi\sum_{j=0}^{\infty}(-1)^j(2j+1)A_{2j+1}K_{2j+1}(w), \quad \star && \text{(D.6o)}\\
&= (-1)^{n+1}\frac{p_{2n+1}}{\pi\sqrt{q}A_1^2}\sum_{j=0}^{\infty} A_{2j+1}\left[I_j(v_1)K_{j+1}(v_2) + I_{j+1}(v_1)K_j(v_2)\right] && \text{(D.6p)}
\end{aligned}
$$

## D.5 Derivatives of the Mathieu functions

### D.5.1 Derivatives for the Angular functions

Exact expressions for the derivatives were obtained by deriving term by term the corresponding series for the Mathieu functions. From Eqs. (2.3)-(2.6)

$$\frac{d}{d\eta}\left[ce_{2n}(\eta;q)\right] = -\sum_{j=0}^{\infty}(2j)A_{2j}\sin 2j\eta \tag{D.7a}$$

$$\frac{d}{d\eta}\left[ce_{2n+1}(\eta;q)\right] = -\sum_{j=0}^{\infty}(2j+1)A_{2j+1}\sin(2j+1)\eta \tag{D.7b}$$

$$\frac{d}{d\eta}\left[se_{2n+2}(\eta;q)\right] = \sum_{j=0}^{\infty}(2j+2)B_{2j+2}\cos(2j+2)\eta \tag{D.7c}$$

$$\frac{d}{d\eta}\left[se_{2n+1}(\eta;q)\right] = \sum_{j=0}^{\infty}(2j+1)B_{2j+1}\cos(2j+1)\eta \tag{D.7d}$$

### D.5.2 Derivatives of the Radial functions of the first kind

The derivatives were obtained by derivating term by term the Bessel function series Eqs. (D.3b), (D.3g), (D.3k) and (D.3n), and using the identity for the Bessel functions $J'_m(x) = \frac{1}{2}\left[J_{m-1}(x) - J_{m+1}(x)\right]$.

$$\frac{d}{d\xi}Je_{2n}(\xi;q) = \frac{ce_{2n}(q,0)}{A_0}\frac{w}{2}\sum_{j=0}^{\infty}A_{2j}\left[J_{2j-1}(u) - J_{2j+1}(u)\right] \tag{D.8a}$$

$$\frac{d}{d\xi}Je_{2n+1}(\xi;q) = \frac{ce'_{2n+1}(q,\frac{\pi}{2})}{A_1}\sinh\xi\sum_{j=0}^{\infty}(-1)^{j+1}A_{2j+1}\left[J_{2j}(w) - J_{2j+2}(w)\right] \tag{D.8b}$$

$$\begin{aligned}\frac{d}{d\xi}Jo_{2n+2}(\xi;q) &= \frac{se'_{2n+2}(q,\frac{\pi}{2})}{B_2}\frac{2}{w}\sum_{j=0}^{\infty}(-1)^{j+1}B_{2j+2} \\ &\quad\times\left\{\left[1+(2j+2)\sinh^2\xi\right]J_{2j+1}(w) + \left[1-(2j+2)\sinh^2\xi\right]J_{2j+3}(w)\right\}\end{aligned} \tag{D.8c}$$

$$\frac{d}{d\xi}Jo_{2n+1}(\xi;q) = \frac{se'_{2n+1}(q,0)}{B_1}\cosh\xi\sum_{j=0}^{\infty}B_{2j+1}\left[J_{2j}(u) - J_{2j+2}(u)\right] \tag{D.8d}$$

### D.5.3 Derivatives of the Radial functions of the second kind

We obtained the derivatives for the RMFs of the second kind from the Bessel function product series in Eqs. (A.9) and (A.11), and using the Bessel identities

$$\begin{aligned} xJ'_n(x) &= xJ_{n-1}(x) - nJ_n(x), \\ xJ'_n(x) &= nJ_n(x) - xJ_{n+1}(x), \\ J'_n(x) &= \frac{1}{2}\left[J_{n-1}(x) - J_{n+1}(x)\right], \end{aligned}$$

$$Ne'_{2n}(\xi) = \frac{p_{2n}}{A_0^2}\sum_{j=0}^{\infty}(-1)^j A_{2j}\left[v_1 J_{j+1}(v_1)N_j(v_2) - v_2 J_j(v_1)N_{j+1}(v_2)\right], \tag{D.9a}$$

$$Ne'_{2n+1}(\xi) = -\frac{p_{2n+1}}{\sqrt{q}A_1^2}\sum_{j=0}^{\infty}(-1)^j A_{2j+1}\times\left\{\begin{array}{c}(v_2-v_1)\left[J_j(v_1)N_j(v_2) - J_{j+1}(v_1)N_{j+1}(v_2)\right]\\ +(2j+1)\left[J_{j+1}(v_1)N_j(v_2) - J_j(v_1)N_{j+1}(v_2)\right]\end{array}\right\}, \tag{D.9b}$$

$$No'_{2n+2}(\xi) = \frac{s_{2n+2}}{qB_2^2}\sum_{j=0}^{\infty}(-1)^{j+1}B_{2j+2}\,(4j+4)\times\left\{\begin{array}{c}J_j(v_1)N_j(v_2) + \cosh(2\xi)J_{j+1}(v_1)N_{j+1}(v_2)\\ -(j+1)\left[\frac{1}{v_1}J_{j+1}(v_1)N_j(v_2) + \frac{1}{v_2}J_j(v_1)N_{j+1}(v_2)\right]\end{array}\right\} \tag{D.9c}$$

$$No'_{2n+1}(\xi) = \frac{s_{2n+1}}{\sqrt{q}B_1^2}\sum_{j=0}^{\infty}(-1)^j B_{2j+1}\times\left\{\begin{array}{c}(v_1+v_2)\left[J_j(v_1)N_j(v_2) + J_{j+1}(v_1)N_{j+1}(v_2)\right]\\ -(2j+1)\left[J_{j+1}(v_1)N_j(v_2) + J_j(v_1)N_{j+1}(v_2)\right]\end{array}\right\} \tag{D.9d}$$

$$Ke'_{2n}(\xi,-q) = (-1)^{n+1}\frac{p_{2n}}{\pi A_0^2}\sum_{j=0}^{\infty}A_{2j}\left[v_2 I_j(v_1)K_{j-1}(v_2) + v_1 I_{j-1}(v_1)K_j(v_2)\right], \tag{D.10a}$$

$$Ke'_{2n+1}(\xi,-q) = (-1)^{n+1}\frac{s_{2n+1}}{\pi\sqrt{q}B_1^2}\sum_{j=0}^{\infty}B_{2j+1}\times\left\{\begin{array}{c}(v_2-v_1)\left[I_j(v_1)K_j(v_2) - I_{j+1}(v_1)K_{j+1}(v_2)\right]\\ +(2j+1)\left[I_{j+1}(v_1)K_j(v_2) + I_j(v_1)K_{j+1}(v_2)\right]\end{array}\right\}, \tag{D.10b}$$

$$Ko'_{2n+2}(\xi,-q) = (-1)^{n+1}\frac{s_{2n+2}}{\pi qB_2^2}\sum_{j=0}^{\infty}B_{2j+2}\,(4j+4)\times\left\{\begin{array}{c}I_j(v_1)K_j(v_2) - \cosh(2\xi)I_{j+1}(v_1)K_{j+1}(v_2)\\ -(j+1)\left[\frac{1}{v_2}I_j(v_1)N_{j+1}(v_2) - \frac{1}{v_1}J_{j+1}(v_1)N_j(v_2)\right]\end{array}\right\}, \tag{D.10c}$$

$$Ko'_{2n+1}(\xi,-q) = (-1)^{n+1}\frac{p_{2n+1}}{\pi\sqrt{q}A_1^2}\sum_{j=0}^{\infty}A_{2j+1}\times\left\{\begin{array}{c}(v_1+v_2)\left[I_j(v_1)K_j(v_2) + I_{j+1}(v_1)K_{j+1}(v_2)\right]\\ +(2j+1)\left[I_j(v_1)K_{j+1}(v_2) - I_{j+1}(v_1)K_j(v_2)\right]\end{array}\right\} \tag{D.10d}$$

### D.5.4 Special values of AMFs and its derivatives

$$ce_{2n}(0,q) = A_0 + A_2 + A_4 + A_6 + ... \qquad se_{2n+2}(0,q) = 0$$
$$ce_{2n}(\pi/2,q) = A_0 - A_2 + A_4 - A_6 + ... \qquad se_{2n+2}(\pi/2,q) = 0$$
$$ce'_{2n}(0,q) = 0 \qquad se'_{2n+2}(0,q) = 2B_2 + 4B_4 + 6B_6 + ...$$
$$ce'_{2n}(\pi/2,q) = 0 \qquad se'_{2n+2}(\pi/2,q) = -2B_2 + 4B_4 - 6B_6 + ...$$

$$ce_{2n+1}(0,q) = A_1 + A_3 + A_5 + A_7 + ... \qquad se_{2n+1}(0,q) = 0$$
$$ce_{2n+1}(\pi/2,q) = 0 \qquad se_{2n+1}(\pi/2,q) = +B_1 - 3B_3 + 5B_5 - ...$$
$$ce'_{2n+1}(0,q) = 0 \qquad se'_{2n+1}(0,q) = B_1 + 3B_3 + 5B_5 + 7B_7 -$$
$$ce'_{2n+1}(\pi/2,q) = -A_1 + 3A_3 - 5A_5 + ... \qquad se'_{2n+1}(\pi/2,q) = 0$$

# Bibliography


[1] M. Abramowitz and I. Stegun, *Handbook of Mathematical Functions.* (Dover, New York:, 1964)

[2] R. Aldrovandi and P. L. Ferreira, "Quantum pendulum," *Am. J. Phys.,* **48**(8), pp. 660-664, Aug. 1980

[3] F. A. Alhargan, "A complete method for the computation of Mathieu Characteristics Numbers of interger orders," *SIAM Review,* **38**(2), pp. 239-255, June 1996

[4] F. A. Alhargan and S. R. Judah, "Mode charts for confocal annular elliptic resonators," *IEE Proc-Microw. Antennas Propag.*, vol. 143, no. 4, pp. 358-360, Aug. 1996

[5] L. Allen, M. W. Beijesbergen, R. J. C. Spreeuw, and J. P. Woerdman, "Orbital angular momentum of light and the transformation of Laguerre-Gaussian laser modes," *Phys. Rev. A,* **45**(11)**,** pp. 8185-8189, June, 1992.

[6] G. Arfken and H. Weber, *Mathematical Methods for Physicists* (Academic Press, San Diego, 1995), 4th ed.

[7] J. Arlt, K. Dholakia, L. Allen, and M. J. Padgett, "Efficiency of second-harmonic generation with Bessel beams," *Phys. Rev. A,* **60**(3), pp. 2438-2441, Sept. 1999

[8] B. Bélanger, P.Y. Fortin, N. Tovmasyan, and M. Piché, "Optical characterization of linear and nonlinear materials using Bessel beams," *SPIE Conference on Optical Beam Characterization,* vol. 3418, pp. 2-10, Quebec Canada, July. 1998

[9] A. K. Bhattacharyya and L. Shafai, "Theoretical and experimental investigation of the elliptical annual ring antenna," *IEEE Trans. Antennas Propagat.,* vol. **AP**-36, no. 11, pp. 1526-1530, Nov. 1988

[10] G. Blanch, "On the computation of Mathieu functions," *J. Math. Phys.,* **25**(1), pp. 1-20, 1946

[11] G. Blanch, "The asymptotic expansions for the odd periodic Mathieu functions," *Trans. Am. Math. Soc.,* **97**(11), pp. 357-366, Nov. 1960

[12] G. Blanch, "Numerical Evaluation of Continued Fractions," *SIAM Review,* **6**(4), pp. 383-421, Oct. 1964

[13] M. Born and E. Wolf, *Principles of Optics* (Cambridge University Press, Cambridge, 1999), 7th. ed.

[14] T. R. Carver, "Mathieu's functions and electrons in a periodic lattice," *Am. J. Phyis.,* **39(**10), pp. 1225-1230, Oct. 1971

[15] D. Clemm, "Algorithm 352 Characteristic values and associated solutions of Mathieu's differential equation," *Comm. of the ACM,* **12**(7), pp.399-408, July 1969

[16] Shan-Chieh Chang, Jianming Jin, Shanjie Zhang, and Jian-Ming Jin, *Computation of Special Functions,* (John Wiley 1996)

[17] S. Chávez-Cerda, G.S. McDonald, and G.H.C. New, "Nondiffracting beams: travelling, standing, rotating and spiral waves," *Opt. Comm.,* **123**, pp. 225-233, 1996

[18] S. Chávez-Cerda, "A new approach to Bessel beams," *J. Modern Opt.*, **46**(6), pp. 923-930, June 1999

[19] S. Chávez-Cerda, M.A. Meneses-Nava, and J. M. Hickmann, "Interference of travelling nondiffracting beams," *Opt. Lett.,* **23**(24), pp. 1871-1873, Dec. 1998

[20] S. Chávez-Cerda, M.A. Meneses-Nava, and J. M. Hickmann, "Reply to Comment on 'Interference of travelling nondiffracting beams'," *Opt. Lett.,* **25**(2), pp. 83-84, Jan. 2000

[21] S. Chávez-Cerda, E. Tepichín, M.A. Meneses-Nava, G. Ramírez, and J. M. Hickmann, "Experimental observation of interfering Bessel beams," *Opt. Exp.,* **3**(13), pp. 524-529, Dec. 1998

[22] S. Chávez-Cerda and G.H.C. New, "Evolution of focused Hankel waves and Bessel beams," *Opt. Comm.,* **181,** pp. 369-378, 15 July 2000

[23] S. Chávez-Cerda, "Self-confined beam propagation and pattern formation in nonlinear optics," *Ph. D. Thesis,* Imperial College, England, 1994.

[24] S. Chávez-Cerda, J. Rogel-Salazar, G. H. C. New, "Bessel beam optical resonator," Submitted to *Opt. Comm.* Nov. 2000.

[25] P. H. Cerpeley, "Rotating waves," *Am. J. Phys.*, **60**(10), pp. 938-942, Oct. 1992

[26] R. Courant and D. Hilbert, *Methods of Mathematical Physics,* (John Wiley & Sons, New York, 1966), vol. 2.

[27] A. Erdélyi, *Bateman manuscript project on higher transcendental functions,* (McGraw-Hill, Malabar Florida, 1981), 1st. reprint ed.

[28] H. Früchting, "Fourier Coefficients of Mathieu Functions in Stable Regions," *J. of Research of Nac. Bureau of Standards,* **73B**(1), pp. 21-24, Jan. 1965

[29] S. Goldstein, "On the asymtotic expansion of the characteristic number of the Mathieu equation," *Proc. Roy. Soc. Edim.*, **49**, pp. 203-223, 1929

[30] S. Goldstein, "Approximate solutions of linear differential equations of the second order , with application to the Mathieu equation," *Proc. London Math. Soc.,* **28**(2)**,** pp. 81-90, 1927

[31] S. Goldstein, "The free oscillations of water in a canal of elliptic plan," *Proc. London Math. Soc.,* **28**(2)**,** pp. 91-101, 1927

[32] J. W. Goodman, *Introduction to Fourier Optics,* (Mc-Graw Hill, New York, 1996), 2nd. ed.

[33] I. S. Gradshteyn and I. M. Ryzhik. *Table of Integrals, Series, and Products* (Academic Press, San Diego, 1994), 5th ed.

[34] P. L. Greene and D. G. Hall, "Properties and diffaction of vector Bessel-Gauss beams," *JOSA A*, **15**(12), pp. 3020-3027, Dec. 1998

[35] P. L. Greene and D. G. Hall, "Focal shift in vector beams," *Opt. Exp.,* **4**(10), pp. 411-419, May 1999

[36] J. C. Gutiérrez-Vega, S. Chávez-Cerda and R. M. Rodríguez-Dagnino, "Free oscillations in an elliptic membrane," *Rev. Mex. Fis.,* **45**(6)**,** pp. 613-622, Dec. 1999

[37] J. C. Gutiérrez-Vega, R.M. Rodríguez-Dagnino and S. Chávez-Cerda, "Attenuation Characteristics in Confocal Annular Elliptic Waveguides and Resonators," Submitted to *IEEE Trans. Microwave Theory Tech.,* March., 2000

[38] J. C. Gutiérrez-Vega, R.M. Rodríguez-Dagnino and S. Chávez-Cerda, "Distribuciones de probabilidad clásicas y cuánticas en billares elípticos," *XLII Congreso Nacional de Física, (7SB5),* Villahermosa México, Nov. 1999.

[39] J. C. Gutiérrez-Vega, M. D. Iturbe-Castillo, and S. Chávez-Cerda, "Alternative formulation for invariant optical fields: Mathieu beams," *Opt. Lett.,* **25**(20)**,** pp. 1493-1495, Oct. 15, 2000

[40] J. C. Gutiérrez-Vega, M. D. Iturbe-Castillo, E. Tepichin, G. Ramírez, S. Chávez-Cerda, and R. M. Rodríguez-Dagnino, "New Member in the Family of Propagation Invariant Optical Fields: Mathieu beams," *Opt. and Phot. News*, **11(**12**),** pp. 35-36, Dec. 2000

[41] J. C. Gutiérrez-Vega, R. Rodríguez-Dagnino, D. Iturbe-Castillo, and S. Chávez-Cerda, "A new class of nondiffracting beams: Mathieu beams," *SPIE Photonics West*, LASE 2001 (LA-4271-08), San José CA, Jan. 2001

[42] A. A. Inayat-Hussain, "Mathieu integral transforms," *J. Math. Phys.,* **32**(3), pp. 669-675, Mar. 1991

[43] E. L. Ince, "Elliptic cylinder functions of second kind," *Proc. Edinburgh Math. Soc.***, 33,** pp. 2-12, 1915

[44] E. L. Ince, "Researches into the Characteristic Numbers of the Mathieu Equation," *Proc. Roy. Soc. Edim.*, **46**, pp.20-29, 1926

[45] G. Indebetouw, "Nondiffracting optical fields: some remarks on their analysis and synthesis," *JOSA A,* **6**(1) pp. 150-152, Jan. 1989

[46] G. Indebetouw, "Polychromatic self-imaging," *J. Mod. Opt.,* **35**(2) pp. 243-252, 1988

[47] J. D. Jackson, *Classical electrodynamics,* (John Wiley & Sons, New York:, 1999), 3rd. ed.

[48] Z. Jaroszewicz, A. Kolodziejczyk, and C. Ramírez, "Comment on 'Interference of travelling nondiffracting beams'," *Opt. Lett.,* **25**(2), pp. 81-82, Jan. 2000

[49] H. Jeffreys, "The free oscillations of water in an elliptical lake," *Proc. London Math. Soc.,* **23,** pp. 455-473, 1924

[50] E. G. Kalnins and W. Miller, Jr., "Lie theory and separation of variables. Orthogonal R-Separable coordinate systems for the wave equation $\psi_{tt} - \Delta_2\psi = 0$," *J. Math. Phys.* **17**(3), pp. 330–355, Mar. 1976.

[51] W. Leeb, "Algorithm 537 Characteristic values of Mathieu's differential equation," *ACM Trans. Math. Soft.,* **5**(1), pp. 112-117, March, 1979

[52] A. Lindner and Heino Freese, "A new method to compute Mathieu functions," *J. Phys. A: Math. Gen.*, **27**, pp. 5565-5571, 1994

[53] J. Mathews and R. L. Walker, *Mathematical Methods of Physics.* (Benjamin, New York, 1965)

[54] E. Mathieu, "Le mouvement vibratoire d'une membrane de forme elliptique," *Jour. de Math. Pures et Appliquées (Jour. de Liouville)*, **13**, pp. 137-203, 1868

[55] MATLAB Softwave, Version 5.2, The Mathworks Inc. 1997

[56] N.W. McLachlan, *Theory and application of Mathieu functions* (Oxford Press, London, 1951)

[57] P. M. Morse and H. Feshbach, *Methods of Theorerical Physics,* (Mc-Graw Hill, New York, 1953)

[58] W. H. Press, S.A. Teukolsky, W. Vetterling and B. Flaneery, *Numerical Recipes*, (Cambridge University Press, Cambridge UK, 1997), 2nd. ed.

[59] ORIGIN Softwave, Version 5.0

[60] L. Pierce, "Calculation of the eigenvalues of a tridiagonal hermitian matrix," *J. Math. Phys.,* **2**(5), pp. 740-741, Sept. 1961

[61] S. R. Rengarajan and J. E. Lewis, "Mathieu Funtions of Integral Order and Real Arguments," *IEEE Trans. Microw. Theory and Tech.,* **MTT-28**(3), pp. 276-277, March 1980

[62] L. Ruby, "Applications of the Mathieu equation," *Am.J.Phys.,* **64** (1), pp. 39-44, 1996

[63] M. Schneider and J. Marquardt, "Fast Computation of Modified Mathieu Functions Applied to Elliptical Waveguide Problems," *IEEE Trans. Microw. Theory and Tech.,* **MTT-47**(4), pp. 513-516, Apr. 1999

[64] M. Sieber, "Semiclassical Transition from and Elliptical to an Oval Billiard,", *J. Phys. A,* **30**(13), pp. 4563-4596, Jun. 1997

[65] R. B. Shirts, "Algorithm 721 MTIEU1 and MTIEU2: Two subroutines to compute eigenvalues and solutions to Mathieu's diffrential equation for noninteger and integer order," *ACM Trans. Math. Soft.,* **19**(3), pp. 391-406, Sept. 1993

[66] R. Sips, "Représentation asymptotique des fonctions de Mathieu et des fonctions d'onde sphéroidales," *Trans. Am. Math. Soc.,* **66**(1), pp. 93-134, Jan. 1949

[67] R. Sips, "Représentation asymptotique des fonctions de Mathieu et des fonctions d'onde sphéroidales II," *Trans. Am. Math. Soc.,* **90**(2), pp. 340-368, Feb. 1959

[68] J. J. Stammes and B. Spjelkavik, "New method for computing eigenfunctions (Mathieu functions) for scattering by elliptical cylinders," *Pure Appl. Opt.*, **4**(1995), pp. 251-262, 1995

[69] J. A. Stratton, *Electromagnetic Theory.* (Mc-Graw Hill, New York, 1941)

[70] J. Swalen, "Remarks on the Continued Fraction Calculation of Eigenvalues and Eigenvectors," *J. Math. Phys.,* **2**(5), pp. 736-739, Sept. 1961

[71] T. Tamir, "Characteristic Exponents of Mathieu Functions," *Math. of Comput.,* **16,** pp.100-106, 1962

[72] T. Tamir and H. C. Wang, "Characteristic Relations for Nonperiodic Solutions of Matheu's Equation," *J. of Research of Nac. Bureau of Standards,* **69B**(1), pp. 101-119, Jan. 1965

[73] N. Toyama and K. Shogen, "Computation of the value of the even and odd mathieu funtions of order $n$ for a given parameter $s$ and an argument $x$," *IEEE Trans. Ant. and Propagat.,* **AP-32**(5), pp.537-539, May 1994

[74] Y. H. Wang and X. Zhang, "Elliptical Fourier series expansion method together with cutoff frequencies in elliptical optical waveguides," *J. Lightwave Tech.,* **LT-16**(10)**,** pp. 1933-1941, Oct. 1998

[75] E.T. Whittaker and G.N. Watson, *A Course of Modern Analysis* (Cambridge University Press, Westford Mass., Reprint of the fourth ed. from 1927), 1st ed. 1902

[76] S. Zhang and Y. Shen, "Eigenmode sequence for an elliptical waveguide with arbitrary ellipticity," *IEEE Trans. Microwave Theory Tech.*, vol. MTT-43, pp. 227-230, Jan. 1995